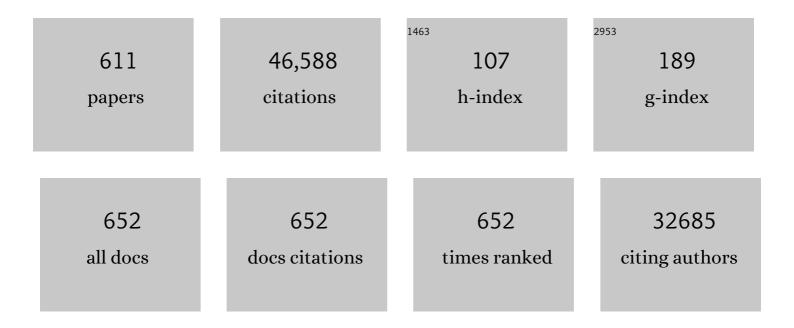
List of Publications by Year in descending order

Source: https://exaly.com/author-pdf/9306358/publications.pdf Version: 2024-02-01



DETED FDATT

#	Article	IF	CITATIONS
1	Nature's hierarchical materials. Progress in Materials Science, 2007, 52, 1263-1334.	32.8	2,254
2	Materials become insensitive to flaws at nanoscale: Lessons from nature. Proceedings of the National Academy of Sciences of the United States of America, 2003, 100, 5597-5600.	7.1	1,641
3	Structure and mechanical quality of the collagen–mineral nano-composite in bone. Journal of Materials Chemistry, 2004, 14, 2115-2123.	6.7	1,081
4	Skeleton of <i>Euplectella</i> sp.: Structural Hierarchy from the Nanoscale to the Macroscale. Science, 2005, 309, 275-278.	12.6	997
5	Iron-Clad Fibers: A Metal-Based Biological Strategy for Hard Flexible Coatings. Science, 2010, 328, 216-220.	12.6	838
6	Mineralized Collagen Fibrils: A Mechanical Model with a Staggered Arrangement of Mineral Particles. Biophysical Journal, 2000, 79, 1737-1746.	0.5	710
7	Biomaterial systems for mechanosensing and actuation. Nature, 2009, 462, 442-448.	27.8	591
8	Nucleation and growth of magnetite from solution. Nature Materials, 2013, 12, 310-314.	27.5	583
9	Cooperative deformation of mineral and collagen in bone at the nanoscale. Proceedings of the National Academy of Sciences of the United States of America, 2006, 103, 17741-17746.	7.1	568
10	Bone mineralization density distribution in health and disease. Bone, 2008, 42, 456-466.	2.9	554
11	The Role of Wheat Awns in the Seed Dispersal Unit. Science, 2007, 316, 884-886.	12.6	541
12	Fibrillar Structure and Mechanical Properties of Collagen. Journal of Structural Biology, 1998, 122, 119-122.	2.8	539
13	Reversible Switching of Hydrogel-Actuated Nanostructures into Complex Micropatterns. Science, 2007, 315, 487-490.	12.6	530
14	Biomimetic materials research: what can we really learn from nature's structural materials?. Journal of the Royal Society Interface, 2007, 4, 637-642.	3.4	501
15	Viscoelastic properties of collagen: synchrotron radiation investigations and structural model. Philosophical Transactions of the Royal Society B: Biological Sciences, 2002, 357, 191-197.	4.0	434
16	Cell-wall recovery after irreversible deformation of wood. Nature Materials, 2003, 2, 810-813.	27.5	427
17	The effect of geometry on three-dimensional tissue growth. Journal of the Royal Society Interface, 2008, 5, 1173-1180.	3.4	413
18	From brittle to ductile fracture of bone. Nature Materials, 2006, 5, 52-55.	27.5	411

#	Article	IF	CITATIONS
19	Validation of quantitative backscattered electron imaging for the measurement of mineral density distribution in human bone biopsies. Bone, 1998, 23, 319-326.	2.9	401
20	Mapping amorphous calcium phosphate transformation into crystalline mineral from the cell to the bone in zebrafish fin rays. Proceedings of the National Academy of Sciences of the United States of America, 2010, 107, 6316-6321.	7.1	389
21	Biological Composites. Annual Review of Materials Research, 2010, 40, 1-24.	9.3	381
22	Size-controlled hydroxyapatite nanoparticles as self-organized organic?inorganic composite materials. Biomaterials, 2005, 26, 5414-5426.	11.4	373
23	Alendronate increases degree and uniformity of mineralization in cancellous bone and decreases the porosity in cortical bone of osteoporotic women. Bone, 2001, 29, 185-191.	2.9	361
24	Nanoscale Deformation Mechanisms in Bone. Nano Letters, 2005, 5, 2108-2111.	9.1	336
25	Actuation systems in plants as prototypes for bioinspired devices. Philosophical Transactions Series A, Mathematical, Physical, and Engineering Sciences, 2009, 367, 1541-1557.	3.4	289
26	Biological composites—complex structures for functional diversity. Science, 2018, 362, 543-547.	12.6	286
27	Architecture of the osteocyte network correlates with bone material quality. Journal of Bone and Mineral Research, 2013, 28, 1837-1845.	2.8	285
28	Radial packing, order, and disorder in collagen fibrils. Biophysical Journal, 1995, 68, 1661-1670.	0.5	281
29	Nucleation and growth of mineral crystals in bone studied by small-angle X-ray scattering. Calcified Tissue International, 1991, 48, 407-413.	3.1	275
30	Geometry as a Factor for Tissue Growth: Towards Shape Optimization of Tissue Engineering Scaffolds. Advanced Healthcare Materials, 2013, 2, 186-194.	7.6	264
31	A customizable software for fast reduction and analysis of large X-ray scattering data sets: applications of the new <i>DPDAK</i> package to small-angle X-ray scattering and grazing-incidence small-angle X-ray scattering. Journal of Applied Crystallography, 2014, 47, 1797-1803.	4.5	244
32	Spiral twisting of fiber orientation inside bone lamellae. Biointerphases, 2006, 1, 1-5.	1.6	241
33	Graded Microstructure and Mechanical Properties of Human Crown Dentin. Calcified Tissue International, 2001, 69, 147-157.	3.1	237
34	Constant mineralization density distribution in cancellous human bone. Bone, 2003, 32, 316-323.	2.9	237
35	Variation of Cellulose Microfibril Angles in Softwoods and Hardwoods—A Possible Strategy of Mechanical Optimization. Journal of Structural Biology, 1999, 128, 257-269.	2.8	234
36	Origami-like unfolding of hydro-actuated ice plant seed capsules. Nature Communications, 2011, 2, 337.	12.8	231

#	Article	IF	CITATIONS
37	The Mechanical Role of Metal Ions in Biogenic Proteinâ€Based Materials. Angewandte Chemie - International Edition, 2014, 53, 12026-12044.	13.8	229
38	Effects of Intermittent Parathyroid Hormone Administration on Bone Mineralization Density in Iliac Crest Biopsies from Patients with Osteoporosis: A Paired Study before and after Treatment. Journal of Clinical Endocrinology and Metabolism, 2003, 88, 1150-1156.	3.6	228
39	Hindered Crack Propagation in Materials with Periodically Varying Young's Modulus—Lessons from Biological Materials. Advanced Materials, 2007, 19, 2657-2661.	21.0	228
40	Mineral crystals in calcified tissues: A comparative study by SAXS. Journal of Bone and Mineral Research, 1992, 7, 329-334.	2.8	224
41	Modeling of Phase Separation in Alloys with Coherent Elastic Misfit. Journal of Statistical Physics, 1999, 95, 1429-1503.	1.2	223
42	Cellulose and collagen: from fibres to tissues. Current Opinion in Colloid and Interface Science, 2003, 8, 32-39.	7.4	206
43	Experimental evidence for a mechanical function of the cellulose microfibril angle in wood cell walls. Philosophical Magazine A: Physics of Condensed Matter, Structure, Defects and Mechanical Properties, 1999, 79, 2173-2184.	0.6	205
44	Mechanical properties of spruce wood cell walls by nanoindentation. Applied Physics A: Materials Science and Processing, 2004, 79, 2069-2073.	2.3	205
45	The bone mineralization density distribution as a fingerprint of the mineralization process. Bone, 2007, 40, 1308-1319.	2.9	204
46	Artful interfaces within biological materials. Materials Today, 2011, 14, 70-78.	14.2	204
47	Bone mineralization in an osteogenesis imperfecta mouse model studied by small-angle x-ray scattering Journal of Clinical Investigation, 1996, 97, 396-402.	8.2	203
48	Two different correlations between nanoindentation modulus and mineral content in the bone–cartilage interface. Journal of Structural Biology, 2005, 149, 138-148.	2.8	196
49	Bone osteonal tissues by Raman spectral mapping: Orientation–composition. Journal of Structural Biology, 2006, 156, 489-496.	2.8	194
50	Collagen fibrils in the human corneal stroma: structure and aging. Investigative Ophthalmology and Visual Science, 1998, 39, 644-8.	3.3	194
51	Collagen fibril orientation in the human corneal stroma and its implication in keratoconus. Investigative Ophthalmology and Visual Science, 1997, 38, 121-9.	3.3	193
52	The organization of the osteocyte network mirrors the extracellular matrix orientation in bone. Journal of Structural Biology, 2011, 173, 303-311.	2.8	192
53	Biological and Biomimetic Materials. Advanced Materials, 2009, 21, 387-388.	21.0	187
54	Scanning Small Angle X-ray Scattering Analysis of Human Bone Sections. Calcified Tissue International, 1999, 64, 422-429.	3.1	177

#	Article	IF	CITATIONS
55	Hierarchical assembly of the siliceous skeletal lattice of the hexactinellid sponge Euplectella aspergillum. Journal of Structural Biology, 2007, 158, 93-106.	2.8	177
56	On the role of interface polymers for the mechanics of natural polymeric composites. Physical Chemistry Chemical Physics, 2004, 6, 5575.	2.8	175
57	Micromechanical properties of biological silica in skeletons of deep-sea sponges. Journal of Materials Research, 2006, 21, 2068-2078.	2.6	171
58	How Linear Tension Converts to Curvature: Geometric Control of Bone Tissue Growth. PLoS ONE, 2012, 7, e36336.	2.5	169
59	Influence of coherency stress on microstructural evolution in model Ni-Al-Mo alloys. Acta Metallurgica Et Materialia, 1995, 43, 1007-1022.	1.8	168
60	Osmotic pressure induced tensile forces in tendon collagen. Nature Communications, 2015, 6, 5942.	12.8	167
61	The Elementary Cellulose Fibril in Picea abies: Comparison of Transmission Electron Microscopy, Small-Angle X-ray Scattering, and Wide-Angle X-ray Scattering Results. Macromolecules, 1995, 28, 8782-8787.	4.8	162
62	Bioinspired Design Criteria for Damageâ€Resistant Materials with Periodically Varying Microstructure. Advanced Functional Materials, 2011, 21, 3634-3641.	14.9	162
63	The grinding tip of the sea urchin tooth exhibits exquisite control over calcite crystal orientation and Mg distribution. Proceedings of the National Academy of Sciences of the United States of America, 2009, 106, 6048-6053.	7.1	161
64	Collagen packing and mineralization. An x-ray scattering investigation of turkey leg tendon. Biophysical Journal, 1993, 64, 260-266.	0.5	153
65	Characteristics of mineral particles in the human bone/cartilage interface. Journal of Structural Biology, 2003, 141, 208-217.	2.8	153
66	A Spider's Fang: How to Design an Injection Needle Using Chitinâ€Based Composite Material. Advanced Functional Materials, 2012, 22, 2519-2528.	14.9	153
67	A hydrated crystalline calcium carbonate phase: Calcium carbonate hemihydrate. Science, 2019, 363, 396-400.	12.6	153
68	The Mechanism of Color Change in the Neon Tetra Fish: a Lightâ€Induced Tunable Photonic Crystal Array. Angewandte Chemie - International Edition, 2015, 54, 12426-12430.	13.8	152
69	A new experimental station for simultaneous X-ray microbeam scanning for small- and wide-angle scattering and fluorescence at BESSY II. Journal of Applied Crystallography, 2006, 40, s466-s470.	4.5	148
70	A materials science vision of extracellular matrix mineralization. Nature Reviews Materials, 2016, 1, .	48.7	148
71	Self-assembly of amorphous calcium carbonate microlens arrays. Nature Communications, 2012, 3, 725.	12.8	147
72	Complementary information on bone ultrastructure from scanning small angle X-ray scattering and Fourier-transform infrared microspectroscopy. Bone, 1999, 25, 287-293.	2.9	146

PETER FRATZL

#	Article	IF	CITATIONS
73	Collagen from the osteogenesis imperfecta mouse model (oim) shows reduced resistance against tensile stress Journal of Clinical Investigation, 1997, 100, 40-45.	8.2	146
74	Microtexture and Chitin/Calcite Orientation Relationship in the Mineralized Exoskeleton of the American Lobster. Advanced Functional Materials, 2008, 18, 3307-3314.	14.9	145
75	Bone tissue engineering: from bench to bedside. Materials Today, 2012, 15, 430-435.	14.2	144
76	Bone Mineralization as Studied by Small-Angle X-Ray Scattering. Connective Tissue Research, 1996, 34, 247-254.	2.3	143
77	Mechanical modulation at the lamellar level in osteonal bone. Journal of Materials Research, 2006, 21, 1913-1921.	2.6	141
78	A new molecular model for collagen elasticity based on synchrotron X-ray scattering evidence. Biophysical Journal, 1997, 72, 1376-1381.	0.5	140
79	Mechanical Function of a Complex Threeâ€Dimensional Suture Joining the Bony Elements in the Shell of the Redâ€Eared Slider Turtle. Advanced Materials, 2009, 21, 407-412.	21.0	139
80	The mechanics of tessellations – bioinspired strategies for fracture resistance. Chemical Society Reviews, 2016, 45, 252-267.	38.1	139
81	Raman imaging of two orthogonal planes within cortical bone. Bone, 2007, 41, 456-461.	2.9	137
82	Plants control the properties and actuation of their organs through the orientation of cellulose fibrils in their cell walls. Integrative and Comparative Biology, 2009, 49, 69-79.	2.0	137
83	Decreased Bone Turnover and Deterioration of Bone Structure in Two Cases of Pycnodysostosis. Journal of Clinical Endocrinology and Metabolism, 2004, 89, 1538-1547.	3.6	136
84	Structural Development of the Mineralized Tissue in the Human L4 Vertebral Body. Journal of Structural Biology, 2001, 136, 126-136.	2.8	135
85	Complementary Information on In Vitro Conversion of Amorphous (Precursor) Calcium Phosphate to Hydroxyapatite from Raman Microspectroscopy and Wide-Angle X-Ray Scattering. Calcified Tissue International, 2006, 79, 354-359.	3.1	134
86	Effects of Laminate Architecture on Fracture Resistance of Sponge Biosilica: Lessons from Nature. Advanced Functional Materials, 2008, 18, 1241-1248.	14.9	132
87	Particle Accretion Mechanism Underlies Biological Crystal Growth from an Amorphous Precursor Phase. Advanced Functional Materials, 2014, 24, 5420-5426.	14.9	132
88	Cortical bone composition and orientation as a function of animal and tissue age in mice by Raman spectroscopy. Bone, 2010, 47, 392-399.	2.9	131
89	Structural transformation of collagen fibrils in corneal stroma during drying. An x-ray scattering study. Biophysical Journal, 1993, 64, 1210-1214.	0.5	130
90	Formation and Structure of Gel Networks from Si(OEt)4/(MeO)3Si(CH2)3NRâ€~2Mixtures (NRâ€~2= NH2or) T	i etq <u>q</u> 0 0 0	rgBT /Overloo

6

#	Article	IF	CITATIONS
91	Collagen: Structure and Mechanics, an Introduction. , 2008, , 1-13.		130
92	Abnormal bone mineralization after fluoride treatment in osteoporosis: A small-angle x-ray-scattering study. Journal of Bone and Mineral Research, 1994, 9, 1541-1549.	2.8	128
93	Modelling of kinetics in multi-component multi-phase systems with spherical precipitatesI: Theory. Materials Science & Engineering A: Structural Materials: Properties, Microstructure and Processing, 2004, 385, 166-174.	5.6	125
94	Collagen insulated from tensile damage by domains that unfold reversibly: In situ X-ray investigation of mechanical yield and damage repair in the mussel byssus. Journal of Structural Biology, 2009, 167, 47-54.	2.8	125
95	Imaging of the helical arrangement of cellulose fibrils in wood by synchrotron X-ray microdiffraction. Journal of Applied Crystallography, 1999, 32, 1127-1133.	4.5	123
96	Small-angle scattering in materials science - a short review of applications in alloys, ceramics and composite materials. Journal of Applied Crystallography, 2003, 36, 397-404.	4.5	123
97	Age- and genotype-dependence of bone material properties in the osteogenesis imperfecta murine model (oim). Bone, 2001, 29, 453-457.	2.9	122
98	Position-Resolved Small-Angle X-ray Scattering of Complex Biological Materials. Journal of Applied Crystallography, 1997, 30, 765-769.	4.5	120
99	Cellulose microfibril orientation of Picea abies and its variability at the micron-level determined by Raman imaging. Journal of Experimental Botany, 2010, 61, 587-595.	4.8	119
100	Diffusion and creep in multi-component alloys with non-ideal sources and sinks for vacancies. Acta Materialia, 2006, 54, 3043-3053.	7.9	117
101	Cellulose fibrils direct plant organ movements. Faraday Discussions, 2008, 139, 275.	3.2	117
102	Enamel-like apatite crown covering amorphous mineral in a crayfish mandible. Nature Communications, 2012, 3, 839.	12.8	116
103	Towards bone replacement materials from calcium phosphates via rapid prototyping and ceramic gelcasting. Materials Science and Engineering C, 2005, 25, 181-186.	7.3	114
104	Multiple roles for neurofibromin in skeletal development and growth. Human Molecular Genetics, 2007, 16, 874-886.	2.9	114
105	Spatial and temporal variations of mechanical properties and mineral content of the external callus during bone healing. Bone, 2009, 45, 185-192.	2.9	114
106	Effects of 3- and 5-Year Treatment With Risedronate on Bone Mineralization Density Distribution in Triple Biopsies of the Iliac Crest in Postmenopausal Women. Journal of Bone and Mineral Research, 2006, 21, 1106-1112.	2.8	112
107	Bone Material Properties in Trabecular Bone From Human Iliac Crest Biopsies After 3- and 5-Year Treatment With Risedronate. Journal of Bone and Mineral Research, 2006, 21, 1581-1590.	2.8	112
108	Lathyrism-induced alterations in collagen cross-links influence the mechanical properties of bone material without affecting the mineral. Bone, 2011, 49, 1232-1241.	2.9	112

#	Article	IF	CITATIONS
109	Tough Lessons From Bone: Extreme Mechanical Anisotropy at the Mesoscale. Advanced Functional Materials, 2008, 18, 1905-1911.	14.9	110
110	Strontium is incorporated into mineral crystals only in newly formed bone during strontium ranelate treatment. Journal of Bone and Mineral Research, 2010, 25, 968-975.	2.8	108
111	Scaling functions, self-similarity, and the morphology of phase-separating systems. Physical Review B, 1991, 44, 4794-4811.	3.2	107
112	The interpretation of structure functions in quenched binary alloys. Acta Metallurgica, 1983, 31, 1849-1860.	2.1	106
113	On the mineral in collagen of human crown dentine. Biomaterials, 2010, 31, 5479-5490.	11.4	106
114	Gains and losses of coral skeletal porosity changes with ocean acidification acclimation. Nature Communications, 2015, 6, 7785.	12.8	106
115	Size and Arrangement of Elementary Cellulose Fibrils in Wood Cells: A Small-Angle X-Ray Scattering Study of Picea abies. Journal of Structural Biology, 1994, 113, 13-22.	2.8	105
116	Microtensile Testing of Wood Fibers Combined with Video Extensometry for Efficient Strain Detection. Holzforschung, 2003, 57, 661-664.	1.9	105
117	Mineralization of cancellous bone after alendronate and sodium fluoride treatment: A quantitative backscattered electron imaging study on minipig ribs. Bone, 1997, 20, 393-397.	2.9	103
118	Stress generation in the tension wood of poplar is based on the lateral swelling power of the Gâ€layer. Plant Journal, 2008, 56, 531-538.	5.7	103
119	The small world of osteocytes: connectomics of the lacuno-canalicular network in bone. New Journal of Physics, 2017, 19, 073019.	2.9	103
120	Tensile forces drive a reversible fibroblast-to-myofibroblast transition during tissue growth in engineered clefts. Science Advances, 2018, 4, eaao4881.	10.3	102
121	The Crystallization of Amorphous Calcium Carbonate is Kinetically Governed by Ion Impurities and Water. Advanced Science, 2018, 5, 1701000.	11.2	101
122	Tensile and compressive stresses in tracheids are induced by swelling based on geometrical constraints of the wood cell. Planta, 2007, 226, 981-987.	3.2	100
123	Diffusion in multi-component systems with no or dense sources and sinks for vacancies. Acta Materialia, 2002, 50, 1369-1381.	7.9	99
124	Early stages of precipitate rafting in a single crystal NiAlMo model alloy investigated by small-angle X-ray scattering and TEM. Acta Materialia, 1997, 45, 1085-1097.	7.9	98
125	Formation and Structure of Porous Gel Networks from Si(OMe)4in the Presence of A(CH2)nSi(OR)3(A) Tj ETQq1	1	l4rgBT /Ovel
126	Evidence for an elementary process in bone plasticity with an activation enthalpy of 1 eV. Journal of the Royal Society Interface, 2007, 4, 277-282.	3.4	97

#	Article	IF	CITATIONS
127	Mechanical adaptation of biological materials — The examples of bone and wood. Materials Science and Engineering C, 2011, 31, 1164-1173.	7.3	97
128	Porous scaffold architecture guides tissue formation. Journal of Bone and Mineral Research, 2012, 27, 1275-1288.	2.8	97
129	Direct Observation of Microfibril Arrangement in a Single Native Cellulose Fiber by Microbeam Small-Angle X-ray Scattering. Macromolecules, 1998, 31, 3953-3957.	4.8	96
130	Improving the osteointegration and bone–implant interface by incorporation of bioactive particles in sol–gel coatings of stainless steel implants. Acta Biomaterialia, 2010, 6, 1601-1609.	8.3	96
131	Inorganicâ ^{~°} Organic Hybrid Polymers by Polymerization of Methacrylate- or Acrylate-Substituted Oxotitanium Clusters with Methyl Methacrylate or Methacrylic Acid. Chemistry of Materials, 2002, 14, 2732-2740.	6.7	93
132	When the cracks begin to show. Nature Materials, 2008, 7, 610-612.	27.5	93
133	Tilted cellulose arrangement as a novel mechanism for hygroscopic coiling in the stork's bill awn. Journal of the Royal Society Interface, 2012, 9, 640-647.	3.4	92
134	Fibrillar level fracture in bone beyond the yield point. International Journal of Fracture, 2006, 139, 425-436.	2.2	90
135	Hydration Dependence of the Wood-Cell Wall Structure inPicea abies.A Small-Angle X-ray Scattering Study. Macromolecules, 1996, 29, 8435-8440.	4.8	89
136	Capillarity-driven deformation of ordered nanoporous silica. Applied Physics Letters, 2009, 95, 083121.	3.3	89
137	Modelling of kinetics in multi-component multi-phase systems with spherical precipitatesII: Numerical solution and application. Materials Science & Engineering A: Structural Materials: Properties, Microstructure and Processing, 2004, 385, 157-165.	5.6	89
138	Pamidronate does not adversely affect bone intrinsic material properties in children with osteogenesis imperfecta. Bone, 2006, 39, 616-622.	2.9	88
139	Designing biomimetic scaffolds for bone regeneration: why aim for a copy of mature tissue properties if nature uses a different approach?. Soft Matter, 2010, 6, 4976.	2.7	88
140	Calcite Crystal Growth by a Solidâ€State Transformation of Stabilized Amorphous Calcium Carbonate Nanospheres in a Hydrogel. Angewandte Chemie - International Edition, 2013, 52, 4867-4870.	13.8	88
141	Biomimetic mineral-organic composite scaffolds with controlled internal architecture. Journal of Materials Science: Materials in Medicine, 2005, 16, 1111-1119.	3.6	86
142	Macromolecular recognition directs calcium ions to coccolith mineralization sites. Science, 2016, 353, 590-593.	12.6	86
143	Structures in the cell wall that enable hygroscopic movement of wheat awns. Journal of Structural Biology, 2008, 164, 101-107.	2.8	84
144	Observations of Multiscale, Stress-Induced Changes of Collagen Orientation in Tendon by Polarized Raman Spectroscopy. Biomacromolecules, 2011, 12, 3989-3996.	5.4	83

#	Article	IF	CITATIONS
145	Intrafibrillar plasticity through mineral/collagen sliding is the dominant mechanism for the extreme toughness of antler bone. Journal of the Mechanical Behavior of Biomedical Materials, 2013, 28, 366-382.	3.1	83
146	A Comparison of Two Techniques for Wood Fibre Isolation ―Evaluation by Tensile Tests on Single Fibres with Different Microfibril Angle. Plant Biology, 2002, 4, 9-12.	3.8	82
147	Inhomogeneous fibril stretching in antler starts after macroscopic yielding: Indication for a nanoscale toughening mechanism. Bone, 2009, 44, 1105-1110.	2.9	82
148	Mineralization density distribution of postmenopausal osteoporotic bone is restored to normal after long-term alendronate treatment: qBEI and sSAXS data from the fracture intervention trial long-term extension (FLEX). Journal of Bone and Mineral Research, 2010, 25, 48-55.	2.8	82
149	Self-Assembled Collagenâ^'Apatite Matrix with Bone-like Hierarchy. Chemistry of Materials, 2010, 22, 3307-3309.	6.7	81
150	Opposite Particle Size Effect on Amorphous Calcium Carbonate Crystallization in Water and during Heating in Air. Chemistry of Materials, 2015, 27, 4237-4246.	6.7	80
151	Surface tension determines tissue shape and growth kinetics. Science Advances, 2019, 5, eaav9394.	10.3	80
152	Effects of sodium fluoride and alendronate on the bone mineral in minipigs: A small-angle X-ray scattering and backscattered electron imaging study. Journal of Bone and Mineral Research, 1996, 11, 248-253.	2.8	79
153	Biomimetics and Biotemplating of Natural Materials. MRS Bulletin, 2010, 35, 219-225.	3.5	79
154	Moisture changes in the plant cell wall force cellulose crystallites to deform. Journal of Structural Biology, 2010, 171, 133-141.	2.8	79
155	Synchrotron Diffraction Study of Deformation Mechanisms in Mineralized Tendon. Physical Review Letters, 2004, 93, 158101.	7.8	78
156	Fragility of Bone Material Controlled by Internal Interfaces. Calcified Tissue International, 2015, 97, 201-212.	3.1	78
157	Modelling of kinetics in multi-component multi-phase systems with spherical precipitates. Materials Science & Engineering A: Structural Materials: Properties, Microstructure and Processing, 2004, 385, 166-174.	5.6	77
158	Kinetics of interfaces during diffusional transformations1F. D. Fischer dedicates this paper to Prof. D. Gross, Darmstadt, on the occasion of his 60th anniversary.1. Acta Materialia, 2001, 49, 1249-1259.	7.9	76
159	Bone material properties in premenopausal women with idiopathic osteoporosis. Journal of Bone and Mineral Research, 2012, 27, 2551-2561.	2.8	76
160	Multiscale structural gradients enhance the biomechanical functionality of the spider fang. Nature Communications, 2014, 5, 3894.	12.8	76
161	Combination of Nanoindentation and Quantitative Backscattered Electron Imaging Revealed Altered Bone Material Properties Associated with Femoral Neck Fragility. Calcified Tissue International, 2009, 85, 335-343.	3.1	75
162	On the Stability of Amorphous Minerals in Lobster Cuticle. Advanced Materials, 2009, 21, 4011-4015.	21.0	74

#	Article	IF	CITATIONS
163	On the pathway of mineral deposition in larval zebrafish caudal fin bone. Bone, 2015, 75, 192-200.	2.9	74
164	Osteoblastic lysosome plays a central role in mineralization. Science Advances, 2019, 5, eaax0672.	10.3	74
165	Matrix mineralization in MC3T3-E1 cell cultures initiated by Î ² -glycerophosphate pulse. Bone, 1998, 23, 511-520.	2.9	73
166	Differential effects of alendronate treatment on bone from growing osteogenesis imperfecta and wild-type mouse. Bone, 2005, 36, 150-158.	2.9	73
167	Rapid alterations of avian medullary bone material during the daily egg-laying cycle. Bone, 2014, 69, 109-117.	2.9	73
168	Characterization of bone mineral crystals in horse radius by small-angle X-ray scattering. Calcified Tissue International, 1996, 58, 341-346.	3.1	72
169	Structural purity of magnetite nanoparticles in magnetotactic bacteria. Journal of the Royal Society Interface, 2011, 8, 1011-1018.	3.4	72
170	Self-similar mesostructure evolution of the growing mollusc shell reminiscent of thermodynamically driven grain growth. Nature Materials, 2014, 13, 1102-1107.	27.5	72
171	Influences of age and mechanical stability on volume, microstructure, and mineralization of the fracture callus during bone healing: Is osteoclast activity the key to age-related impaired healing?. Bone, 2010, 47, 219-228.	2.9	71
172	Cellulose microfibril angles in a spruce branch and mechanical implications. Journal of Materials Science, 2001, 36, 5087-5092.	3.7	70
173	Mineralization generates megapascal contractile stresses in collagen fibrils. Science, 2022, 376, 188-192.	12.6	70
174	Spiral angle of elementary cellulose fibrils in cell walls ofPicea abies determined by small-angle x-ray scattering. Wood Science and Technology, 1998, 32, 335-345.	3.2	69
175	In vitro bioactivity of bioresorbable porous polymeric scaffolds incorporating hydroxyapatite microspheres. Acta Biomaterialia, 2010, 6, 2525-2531.	8.3	69
176	Hierarchical Calcite Crystals with Occlusions of a Simple Polyelectrolyte Mimic Complex Biomineral Structures. Advanced Functional Materials, 2012, 22, 4668-4676.	14.9	69
177	Self-Repair of a Biological Fiber Guided by an Ordered Elastic Framework. Biomacromolecules, 2013, 14, 1520-1528.	5.4	69
178	Improvements of strength and fracture resistance by spatial material property variations. Acta Materialia, 2014, 68, 279-294.	7.9	69
179	The mechanoresponse of bone is closely related to the osteocyte lacunocanalicular network architecture. Proceedings of the National Academy of Sciences of the United States of America, 2020, 117, 32251-32259.	7.1	69
180	Lead accumulation in tidemark of articular cartilage. Osteoarthritis and Cartilage, 2006, 14, 906-913.	1.3	68

#	Article	IF	CITATIONS
181	Scanning texture analysis of lamellar bone using microbeam synchrotron X-ray radiation. Journal of Applied Crystallography, 2007, 40, 115-120.	4.5	68
182	Evidence that Treatment with Risedronate in Women with Postmenopausal Osteoporosis Affects Bone Mineralization and Bone Volume. Calcified Tissue International, 2007, 81, 73-80.	3.1	68
183	Application of the thermodynamic extremal principle to the diffusional phase transformations. Acta Materialia, 2004, 52, 959-967.	7.9	67
184	Effect of Temporal Changes in Bone Turnover on the Bone Mineralization Density Distribution: A Computer Simulation Study. Journal of Bone and Mineral Research, 2008, 23, 1905-1914.	2.8	67
185	Kinetics of spinodal decomposition in the Ising model with vacancy diffusion. Physical Review B, 1994, 50, 3477-3480.	3.2	66
186	Universality of scaled structure functions in quenched systems undergoing phase separation. Acta Metallurgica, 1989, 37, 3245-3248.	2.1	65
187	The physics of tissue patterning and extracellular matrix organisation: how cells join forces. Soft Matter, 2011, 7, 9549.	2.7	65
188	X-ray vector radiography for bone micro-architecture diagnostics. Physics in Medicine and Biology, 2012, 57, 3451-3461.	3.0	65
189	The Use of Smallâ€Angle Xâ€Ray Diffraction Studies for the Analysis of Structural Features in Archaeological Samples. Archaeometry, 2001, 43, 117-129.	1.3	64
190	The implication of chemical extraction treatments on the cell wall nanostructure of softwood. Cellulose, 2008, 15, 407.	4.9	64
191	Elastic response of mesoporous silicon to capillary pressures in the pores. Applied Physics Letters, 2015, 106, .	3.3	64
192	Bone mineralization pathways during the rapid growth of embryonic chicken long bones. Journal of Structural Biology, 2016, 195, 82-92.	2.8	64
193	A thermodynamic approach to grain growth and coarsening. Philosophical Magazine, 2003, 83, 1075-1093.	1.6	63
194	Multilevel architectures in natural materials. Scripta Materialia, 2013, 68, 8-12.	5.2	63
195	Bone material quality in transiliac bone biopsies of postmenopausal osteoporotic women after 3 years of strontium ranelate treatment. Journal of Bone and Mineral Research, 2010, 25, 891-900.	2.8	62
196	Mineral Formation in the Larval Zebrafish Tail Bone Occurs via an Acidic Disordered Calcium Phosphate Phase. Journal of the American Chemical Society, 2016, 138, 14481-14487.	13.7	62
197	Scaffold curvature-mediated novel biomineralization process originates a continuous soft tissue-to-bone interface. Acta Biomaterialia, 2017, 60, 64-80.	8.3	62
198	Cross-Linking of Poly(methyl methacrylate) by the Methacrylate-Substituted Oxozirconium Cluster Zr6(OH)4O4(Methacrylate)12. Chemistry of Materials, 2000, 12, 602-604.	6.7	61

#	Article	IF	CITATIONS
199	Size and habit of mineral particles in bone and mineralized callus during bone healing in sheep. Journal of Bone and Mineral Research, 2010, 25, 2029-2038.	2.8	61
200	Selecting for Function: Solution Synthesis of Magnetic Nanopropellers. Nano Letters, 2013, 13, 5373-5378.	9.1	61
201	Polarized Raman Anisotropic Response of Collagen in Tendon: Towards 3D Orientation Mapping of Collagen in Tissues. PLoS ONE, 2013, 8, e63518.	2.5	61
202	Mineral particle size in children with osteogenesis imperfecta type I is not increased independently of specific collagen mutations. Bone, 2014, 60, 122-128.	2.9	61
203	Fast Magnetic Micropropellers with Random Shapes. Nano Letters, 2015, 15, 7064-7070.	9.1	61
204	Structure?function relationships of four compression wood types: micromechanical properties at the tissue and fibre level. Trees - Structure and Function, 2004, 18, 480.	1.9	60
205	G-fibres in storage roots of <i>Trifolium pratense</i> (Fabaceae): tensile stress generators for contraction. Plant Journal, 2010, 61, 854-861.	5.7	60
206	Identification of root filling interfaces by microscopy and tomography methods. International Endodontic Journal, 2011, 44, 395-401.	5.0	60
207	An Alternative Route Towards Metal–Polymer Hybrid Materials Prepared by Vaporâ€Phase Processing. Advanced Functional Materials, 2011, 21, 3047-3055.	14.9	60
208	Guanineâ€Based Photonic Crystals in Fish Scales Form from an Amorphous Precursor. Angewandte Chemie - International Edition, 2013, 52, 388-391.	13.8	60
209	Ultrastructural and developmental features of the tessellated endoskeleton of elasmobranchs (sharks and rays). Journal of Anatomy, 2016, 229, 681-702.	1.5	60
210	Modelling the role of surface stress on the kinetics of tissue growth in confined geometries. Acta Biomaterialia, 2013, 9, 5531-5543.	8.3	59
211	Simultaneous Raman Microspectroscopy and Fluorescence Imaging of Bone Mineralization in Living Zebrafish Larvae. Biophysical Journal, 2014, 106, L17-L19.	0.5	59
212	Title is missing!. Journal of Materials Science, 2001, 36, 4681-4686.	3.7	58
213	The onset of amelogenin nanosphere aggregation studied by small-angle X-ray scattering and dynamic light scattering. Journal of Structural Biology, 2005, 151, 239-249.	2.8	58
214	Crack driving force in twisted plywood structures. Acta Biomaterialia, 2017, 55, 349-359.	8.3	58
215	Mechanical model for the deformation of the wood cell wall. International Journal of Materials Research, 2004, 95, 579-584.	0.8	57
216	Association of COLIA1 Sp1 Alleles with Defective Bone Nodule Formation In Vitro and Abnormal Bone Mineralization In Vivo. Calcified Tissue International, 2005, 77, 113-118.	3.1	57

#	Article	IF	CITATIONS
217	Imaging the Nanostructure of Bone and Dentin Through Small- and Wide-Angle X-Ray Scattering. Methods in Enzymology, 2013, 532, 391-413.	1.0	57
218	Aging Versus Postmenopausal Osteoporosis: Bone Composition and Maturation Kinetics at Actively-Forming Trabecular Surfaces of Female Subjects Aged 1 to 84 Years. Journal of Bone and Mineral Research, 2016, 31, 347-357.	2.8	57
219	Structural Changes during Plastic Deformation at Crack Tips in PVDF Films:Â A Scanning X-ray Scattering Study. Macromolecules, 2005, 38, 6099-6105.	4.8	55
220	SMAD versus Non-SMAD Signaling Is Determined by Lateral Mobility of Bone Morphogenetic Protein (BMP) Receptors. Journal of Biological Chemistry, 2012, 287, 39492-39504.	3.4	55
221	Relationship between the v2PO4/amide III ratio assessed by Raman spectroscopy and the calcium content measured by quantitative backscattered electron microscopy in healthy human osteonal bone. Journal of Biomedical Optics, 2014, 19, 065002.	2.6	55
222	BMP delivery complements the guiding effect of scaffold architecture without altering bone microstructure in critical-sized long bone defects: A multiscale analysis. Acta Biomaterialia, 2015, 23, 282-294.	8.3	55
223	Multiscale characterization of the mineral phase at skeletal sites of breast cancer metastasis. Proceedings of the National Academy of Sciences of the United States of America, 2017, 114, 10542-10547.	7.1	55
224	Pole figure analysis of mineral nanoparticle orientation in individual trabecula of human vertebral bone. Journal of Applied Crystallography, 2003, 36, 494-498.	4.5	54
225	Scanning X-ray imaging with small-angle scattering contrast. Journal of Applied Crystallography, 2007, 40, s78-s82.	4.5	54
226	Multi-scale thermal stability of a hard thermoplastic protein-based material. Nature Communications, 2015, 6, 8313.	12.8	54
227	Cooperative behavior of a sacrificial bond network and elastic framework in providing self-healing capacity in mussel byssal threads. Journal of Structural Biology, 2016, 196, 329-339.	2.8	54
228	Multiscale analyses reveal native-like lamellar bone repair and near perfect bone-contact with porous strontium-loaded bioactive glass. Biomaterials, 2019, 209, 152-162.	11.4	54
229	Nanoengineered Colloidal Probes for Ramanâ€based Detection of Biomolecules inside Living Cells. Small, 2013, 9, 351-356.	10.0	53
230	Compressive Residual Strains in Mineral Nanoparticles as a Possible Origin of Enhanced Crack Resistance in Human Tooth Dentin. Nano Letters, 2015, 15, 3729-3734.	9.1	53
231	Orientation of Mineral Crystallites and Mineral Density During Skeletal Development in Mice Deficient in Tissue Nonspecific Alkaline Phosphatase. Journal of Bone and Mineral Research, 2003, 18, 117-125.	2.8	52
232	Effect of growth rate on mean microfibril angle and cross-sectional shape of tracheids of Norway spruce. Trees - Structure and Function, 2004, 18, 354-362.	1.9	52
233	Two stages in three-dimensional <i>in vitro</i> growth of tissue generated by osteoblastlike cells. Biointerphases, 2010, 5, 45-52.	1.6	52
234	Evaluation of 3D small-angle scattering from non-spherical particles in single crystals. Journal of Applied Crystallography, 1993, 26, 820-826.	4.5	51

#	Article	IF	CITATIONS
235	Crossover from ω-phase to α-phase precipitation in bcc Ti-Mo. Physical Review B, 1994, 49, 11759-11766.	3.2	51
236	Architecturing materials at mesoscale: some current trends. Materials Research Letters, 2021, 9, 399-421.	8.7	51
237	A finite element study on the effects of disorder in cellular structures. Acta Biomaterialia, 2009, 5, 381-390.	8.3	50
238	New Suggestions for the Mechanical Control of Bone Remodeling. Calcified Tissue International, 2009, 85, 45-54.	3.1	50
239	Accelerated Growth Plate Mineralization and Foreshortened Proximal Limb Bones in Fetuin-A Knockout Mice. PLoS ONE, 2012, 7, e47338.	2.5	50
240	Metal-Tunable Self-Assembly of Hierarchical Structure in Mussel-Inspired Peptide Films. ACS Nano, 2018, 12, 2160-2168.	14.6	50
241	Plant Cystoliths: A Complex Functional Biocomposite of Four Distinct Silica and Amorphous Calcium Carbonate Phases. Chemistry - A European Journal, 2012, 18, 10262-10270.	3.3	49
242	Osmotically driven tensile stress in collagen-based mineralized tissues. Journal of the Mechanical Behavior of Biomedical Materials, 2015, 52, 14-21.	3.1	49
243	Fabrication and moulding of cellular materials by rapid prototyping. International Journal of Materials and Product Technology, 2004, 21, 285.	0.2	48
244	<i>In situ</i> observation of cluster formation during nanoparticle solution casting on a colloidal film. Journal of Physics Condensed Matter, 2011, 23, 254208.	1.8	48
245	Magnetite Crystal Orientation in Magnetosome Chains. Advanced Functional Materials, 2014, 24, 3926-3932.	14.9	48
246	Changes in the Degree of Mineralization with Osteoporosis and its Treatment. Current Osteoporosis Reports, 2014, 12, 338-350.	3.6	48
247	Unique micro- and nano-scale mineralization pattern of human osteogenesis imperfecta type VI bone. Bone, 2015, 73, 233-241.	2.9	48
248	Ising model for phase separation in alloys with anisotropic elastic interaction—I. Theory. Acta Metallurgica Et Materialia, 1995, 43, 2921-2930.	1.8	47
249	Targeted Overexpression of Vitamin D Receptor in Osteoblasts Increases Calcium Concentration Without Affecting Structural Properties of Bone Mineral Crystals. Calcified Tissue International, 2003, 73, 251-257.	3.1	47
250	Cellular Solids beyond the Apparent Density– an Experimental Assessment of Mechanical Properties. Advanced Engineering Materials, 2004, 6, 134-138.	3.5	47
251	Analysis of the hierarchical structure of biological tissues by scanning X-ray scattering using a micro-beam. Cellular and Molecular Biology, 2000, 46, 993-1004.	0.9	47
252	3D variations in human crown dentin tubule orientation: A phase-contrast microtomography study. Dental Materials, 2010, 26, e1-e10.	3.5	46

#	Article	IF	CITATIONS
253	Biomimetic Principles in Polymer and Material Science. Macromolecular Chemistry and Physics, 2010, 211, 166-170.	2.2	46
254	Osteoclasts on Bone and Dentin In Vitro: Mechanism of Trail Formation and Comparison of Resorption Behavior. Calcified Tissue International, 2013, 93, 526-539.	3.1	46
255	Pediatric reference Raman data for material characteristics of iliac trabecular bone. Bone, 2014, 69, 89-97.	2.9	46
256	Control of Polymorph Selection in Amorphous Calcium Carbonate Crystallization by Poly(Aspartic) Tj ETQq0 0 0	rgBT /Ove 10:0	rlock 10 Tf 50
257	Sacrificial Ionic Bonds Need To Be Randomly Distributed To Provide Shear Deformability. Nano Letters, 2009, 9, 3603-3607.	9.1	45
258	Scanning small-angle X-ray scattering analysis of the size and organization of the mineral nanoparticles in fluorotic bone using a stack of cards model. Journal of Applied Crystallography, 2010, 43, 1385-1392.	4.5	45
259	Surfactant Self-Assembly in Cylindrical Silica Nanopores. Journal of Physical Chemistry Letters, 2010, 1, 1442-1446.	4.6	45
260	Elastic Effects on Phase Segregation in Alloys with External Stresses. Physical Review Letters, 1995, 75, 4448-4451.	7.8	44
261	Interdependence of strain and shape in self-assembled coherent InAs islands on GaAs. Europhysics Letters, 1999, 45, 222-227.	2.0	44
262	Combined treatment with PTH (1–34) and OPG increases bone volume and uniformity of mineralization in aged ovariectomized rats. Bone, 2005, 37, 87-95.	2.9	44
263	Tissue growth into threeâ€dimensional composite scaffolds with controlled microâ€features and nanotopographical surfaces. Journal of Biomedical Materials Research - Part A, 2013, 101, 2796-2807.	4.0	44
264	A spider's biological vibration filter: Micromechanical characteristics of a biomaterial surface. Acta Biomaterialia, 2014, 10, 4832-4842.	8.3	44
265	Towards a Connectomic Description of the Osteocyte Lacunocanalicular Network in Bone. Current Osteoporosis Reports, 2019, 17, 186-194.	3.6	44
266	Statistical model of the habit and arrangement of mineral crystals in the collagen of bone. Journal of Statistical Physics, 1994, 77, 125-143.	1.2	43
267	Spatial-Temporal Mapping of Bone Structural and Elastic Properties in a Sheep Model Following Osteotomy. Ultrasound in Medicine and Biology, 2011, 37, 474-483.	1.5	43
268	Network architecture strongly influences the fluid flow pattern through the lacunocanalicular network in human osteons. Biomechanics and Modeling in Mechanobiology, 2020, 19, 823-840.	2.8	43
269	Competing mechanisms for precipitate coarsening in phase separation with vacancy dynamics. Physical Review B, 1997, 55, R6101-R6104.	3.2	42
270	Small-Angle X-Ray Scattering to Characterize Nanostructures in Inorganic and Hybrid Materials Chemistry. Monatshefte FÃ1⁄4r Chemie, 2006, 137, 529-543.	1.8	42

#	Article	IF	CITATIONS
271	A theoretical model for tissue growth in confined geometries. Journal of the Mechanics and Physics of Solids, 2010, 58, 1073-1087.	4.8	42
272	Lightâ€Induced Water Splitting Causes Highâ€Amplitude Oscillation of pHâ€Sensitive Layerâ€byâ€Layer Assembl on TiO ₂ . Angewandte Chemie - International Edition, 2016, 55, 13001-13004.	ies 13.8	42
273	Hydrogen Bonding in Amorphous Calcium Carbonate and Molecular Reorientation Induced by Dehydration. Journal of Physical Chemistry C, 2018, 122, 3591-3598.	3.1	42
274	Nano-scale modulus mapping of biological composite materials: Theory and practice. Progress in Materials Science, 2017, 87, 292-320.	32.8	41
275	Correlative imaging reveals physiochemical heterogeneity of microcalcifications in human breast carcinomas. Journal of Structural Biology, 2018, 202, 25-34.	2.8	41
276	Hierarchically-structured metalloprotein composite coatings biofabricated from co-existing condensed liquid phases. Nature Communications, 2020, 11, 862.	12.8	41
277	Structural and mechanical properties of the arthropod cuticle: Comparison between the fang of the spider Cupiennius salei and the carapace of American lobster Homarus americanus. Journal of Structural Biology, 2013, 183, 172-179.	2.8	40
278	Mechanical and structural properties of bone in non-critical and critical healing in rat. Acta Biomaterialia, 2014, 10, 4009-4019.	8.3	40
279	Unraveling the Molecular Requirements for Macroscopic Silk Supercontraction. ACS Nano, 2017, 11, 9750-9758.	14.6	40
280	Model for the structural changes occurring at low temperatures inPdDx. Physical Review B, 1981, 24, 277-282.	3.2	39
281	Gel Structures Containing Al(III). Langmuir, 1999, 15, 6631-6636.	3.5	39
282	Three-dimensional structural interrelations between cells, extracellular matrix, and mineral in normally mineralizing avian leg tendon. Proceedings of the National Academy of Sciences of the United States of America, 2020, 117, 14102-14109.	7.1	39
283	Short-range order in Au-Fe alloys studied by high-temperature Mössbauer spectroscopy. Physical Review B, 1989, 39, 6395-6402.	3.2	38
284	Pore structure of carbon/carbon composites studied by small-angle X-ray scattering. Carbon, 1994, 32, 939-945.	10.3	38
285	Modelling of kinetics in multi-component multi-phase systems with spherical precipitates. Materials Science & Engineering A: Structural Materials: Properties, Microstructure and Processing, 2004, 385, 157-165.	5.6	38
286	Enhanced cellulose orientation analysis in complex model plant tissues. Journal of Structural Biology, 2013, 183, 419-428.	2.8	38
287	Water-Mediated Collagen and Mineral Nanoparticle Interactions Guide Functional Deformation of Human Tooth Dentin. Chemistry of Materials, 2016, 28, 3416-3427.	6.7	38

288 Calcified cartilage or bone? Collagens in the tessellated endoskeletons of cartilaginous fish (sharks) Tj ETQq0 0 0 rgBT /Overlock 10 Tf 5

#	Article	IF	CITATIONS
289	Investigation of bone and cartilage by synchrotron scanning-SAXS and -WAXD with micrometer spatial resolution. Journal of Applied Crystallography, 2000, 33, 820-823.	4.5	37
290	Fresnel-propagated imaging for the study of human tooth dentin by partially coherent x-ray tomography. Optics Express, 2006, 14, 8584.	3.4	37
291	Tubular frameworks guiding orderly bone formation in the antler of the red deer (Cervus elaphus). Journal of Structural Biology, 2011, 175, 457-464.	2.8	37
292	The use of ultrasonic cavitation for near-surface structuring of robust and low-cost AlNi catalysts for hydrogen production. Green Chemistry, 2015, 17, 2745-2749.	9.0	37
293	Gradual conversion of cellular stress patterns into pre-stressed matrix architecture during <i>in vitro</i> tissue growth. Journal of the Royal Society Interface, 2016, 13, 20160136.	3.4	37
294	The internal structure of single carbon fibers determined by simultaneous small- and wide-angle scattering. Journal of Applied Crystallography, 2000, 33, 695-699.	4.5	36
295	Stochastic Lattice Model for Bone Remodeling and Aging. Physical Review Letters, 2004, 93, 228102.	7.8	36
296	The role of material properties for the mechanical adaptation at branch junctions. Trees - Structure and Function, 2009, 23, 605-610.	1.9	36
297	Temporal tissue patterns in bone healing of sheep. Journal of Orthopaedic Research, 2010, 28, 1440-1447.	2.3	36
298	Unifying Design Strategies in Demosponge and Hexactinellid Skeletal Systems. Journal of Adhesion, 2010, 86, 72-95.	3.0	36
299	Evidence for a Role for Nanoporosity and Pyridinoline Content in Human Mild Osteogenesis Imperfecta. Journal of Bone and Mineral Research, 2016, 31, 1050-1059.	2.8	36
300	Properties of chemically and mechanically isolated fibres of spruce (Picea abies[L.] Karst.). Part 2: Twisting phenomena. Holzforschung, 2005, 59, 247-251.	1.9	35
301	Nanostructure of Biogenic Calcite Crystals: A View by Small-Angle X-Ray Scattering. Crystal Growth and Design, 2011, 11, 2054-2058.	3.0	35
302	Pseudoelastic behaviour of a natural material is achieved via reversible changes in protein backbone conformation. Journal of the Royal Society Interface, 2012, 9, 2911-2922.	3.4	35
303	Properties of chemically and mechanically isolated fibres of spruce (Picea abies [L.] Karst.). Part 3: Mechanical characterisation. Holzforschung, 2005, 59, 354-357.	1.9	34
304	Orientation dependent fracture toughness of lamellar bone. International Journal of Fracture, 2006, 139, 395-405.	2.2	34
305	Three-dimensional growth behavior of osteoblasts on biomimetic hydroxylapatite scaffolds. Journal of Biomedical Materials Research - Part A, 2007, 81A, 40-50.	4.0	34
306	The Role of Titanium Surface Nanostructuring on Preosteoblast Morphology, Adhesion, and Migration. Advanced Healthcare Materials, 2017, 6, 1601244.	7.6	34

#	Article	IF	CITATIONS
307	Pattern formation and collective effects in populations of magnetic microswimmers. Journal Physics D: Applied Physics, 2017, 50, 11LT03.	2.8	34
308	Interplay between Calcite, Amorphous Calcium Carbonate, and Intracrystalline Organics in Sea Urchin Skeletal Elements. Crystal Growth and Design, 2018, 18, 2189-2201.	3.0	34
309	The growth of ω-phase inclusions in Ti-20 at.% Mo and the competition between elastic and surface energies. Acta Metallurgica Et Materialia, 1991, 39, 753-761.	1.8	33
310	Measurements of mechanical properties in Ni-base superalloys using nanoindentation and atomic force microscopy. Materials Science & Engineering A: Structural Materials: Properties, Microstructure and Processing, 2003, 363, 211-220.	5.6	33
311	Spinodal Decomposition. , 2005, , 409-480.		33
312	A kinetic model of the transformation of a micropatterned amorphous precursor into a porous single crystal. Acta Biomaterialia, 2010, 6, 1001-1005.	8.3	33
313	Fetal and postnatal mouse bone tissue contains more calcium than is present in hydroxyapatite. Journal of Structural Biology, 2011, 176, 159-167.	2.8	33
314	On the Phase Diagram of Calcium Carbonate Solutions. Advanced Materials Interfaces, 2017, 4, 1600076.	3.7	33
315	The contribution of the pericanalicular matrix to mineral content in human osteonal bone. Bone, 2019, 123, 76-85.	2.9	33
316	Ising model for phase separation in alloys with anisotropic elastic interaction—II. A computer experiment. Acta Materialia, 1996, 44, 3227-3239.	7.9	32
317	Microscopic model for directional coarsening of precipitates in alloys under external load. Acta Materialia, 1997, 45, 3949-3962.	7.9	32
318	Physicochemical Basis for Water-Actuated Movement and Stress Generation in Nonliving Plant Tissues. Physical Review Letters, 2013, 111, 238001.	7.8	32
319	Switching the Stiffness of Polyelectrolyte Assembly by Light to Control Behavior of Supported Cells. Macromolecular Bioscience, 2016, 16, 1422-1431.	4.1	32
320	Amelogenin Nanoparticles in Suspension: Deviations from Spherical Shape and pH-Dependent Aggregation. Biomacromolecules, 2010, 11, 369-376.	5.4	31
321	Micro- and nano-structural details of a spider's filter for substrate vibrations: relevance for low-frequency signal transmission. Journal of the Royal Society Interface, 2015, 12, 20141111.	3.4	31
322	Additives influence the phase behavior of calcium carbonate solution by a cooperative ion-association process. Journal of Materials Chemistry B, 2018, 6, 449-457.	5.8	31
323	Natural load-bearing protein materials. Progress in Materials Science, 2021, 120, 100767.	32.8	31
324	Title is missing!. Journal of Materials Science, 2002, 37, 4279-4284.	3.7	30

#	Article	IF	CITATIONS
325	Structural Adaptation of Trabecular Bone Revealed by Position Resolved Analysis of Proximal Femora of Different Primates. Anatomical Record, 2011, 294, 55-67.	1.4	30
326	An excursion into the design space of biomimetic architectured biphasic actuators. International Journal of Materials Research, 2011, 102, 607-612.	0.3	30
327	Collagen. , 2012, , 35-55.		30
328	In situ elastic modulus measurements of ultrathin protein-rich organic layers in biosilica: towards deeper understanding of superior resistance to fracture of biocomposites. RSC Advances, 2013, 3, 5798.	3.6	30
329	Pressurized honeycombs as soft-actuators: a theoretical study. Journal of the Royal Society Interface, 2014, 11, 20140458.	3.4	30
330	Normal mineralization and nanostructure of sclerotic bone in mice overexpressing Fra-1. Bone, 2004, 34, 776-782.	2.9	29
331	Pore-lattice deformations in ordered mesoporous matrices: experimental studies and theoretical analysis. Physical Chemistry Chemical Physics, 2010, 12, 11267.	2.8	29
332	Poorly Ordered Bone as an Endogenous Scaffold for the Deposition of Highly Oriented Lamellar Tissue in Rapidly Growing Ovine Bone. Cells Tissues Organs, 2011, 194, 119-123.	2.3	29
333	Increased bone remodelling around titanium implants coated with chondroitin sulfate in ovariectomized rats. Acta Biomaterialia, 2014, 10, 2855-2865.	8.3	29
334	Climateâ€Dependent Heatâ€Triggered Opening Mechanism of <i>Banksia</i> Seed Pods. Advanced Science, 2018, 5, 1700572.	11.2	29
335	Wood and the Activity of Dead Tissue. Advanced Materials, 2021, 33, e2001412.	21.0	29
336	Breast cancer–secreted factors perturb murine bone growth in regions prone to metastasis. Science Advances, 2021, 7, .	10.3	29
337	3D Interrelationship between Osteocyte Network and Forming Mineral during Human Bone Remodeling. Advanced Healthcare Materials, 2021, 10, e2100113.	7.6	29
338	Multiscale, Converging Defects of Macro-Porosity, Microstructure and Matrix Mineralization Impact Long Bone Fragility in NF1. PLoS ONE, 2014, 9, e86115.	2.5	29
339	Using Kinetic Monte Carlo simulations to study phase separation in Alloys. Phase Transitions, 2004, 77, 433-456.	1.3	28
340	The mechanical heterogeneity of the hard callus influences local tissue strains during bone healing: A finite element study based on sheep experiments. Journal of Biomechanics, 2011, 44, 517-523.	2.1	28
341	New Materials through Bioinspiration and Nanoscience. Advanced Functional Materials, 2013, 23, 4398-4399.	14.9	28
342	Layered growth of crayfish gastrolith: About the stability of amorphous calcium carbonate and role of additives. Journal of Structural Biology, 2015, 189, 28-36.	2.8	28

#	Article	IF	CITATIONS
343	Small-angle scattering from porous amorphous substances. Journal of Applied Crystallography, 1991, 24, 588-592.	4.5	27
344	By which mechanism does coarsening in phase-separating alloys proceed?. Europhysics Letters, 2003, 61, 261-267.	2.0	27
345	Characterizing moisture-dependent mechanical properties of organic materials: humidity-controlled static and dynamic nanoindentation of wood cell walls. Philosophical Magazine, 2015, 95, 1992-1998.	1.6	27
346	Shear-Induced β-Crystallite Unfolding in Condensed Phase Nanodroplets Promotes Fiber Formation in a Biological Adhesive. ACS Nano, 2019, 13, 4992-5001.	14.6	27
347	Alterations of bone material properties in adult patients with X-linked hypophosphatemia (XLH). Journal of Structural Biology, 2020, 211, 107556.	2.8	27
348	Mineralized Microstructure of Calcified Avian Tendons: A Scanning Small Angle X-ray Scattering Study. Calcified Tissue International, 2003, 72, 567-576.	3.1	26
349	Sonication-Assisted Synthesis of Large, High-Quality Mercury Thiolate Single Crystals Directly from Liquid Mercury. Journal of the American Chemical Society, 2010, 132, 14355-14357.	13.7	26
350	Cooperation of length scales and orientations in the deformation of bovine bone. Acta Biomaterialia, 2011, 7, 2943-2951.	8.3	26
351	Characterizing the transformation near indents and cracks in clinically used dental yttria-stabilized zirconium oxide constructs. Dental Materials, 2013, 29, 241-251.	3.5	26
352	Relationship of Bone Mineralization Density Distribution (BMDD) in Cortical and Cancellous Bone Within the Iliac Crest of Healthy Premenopausal Women. Calcified Tissue International, 2014, 95, 332-339.	3.1	26
353	Exploring mussel byssus fabrication with peptide-polymer hybrids: Role of pH and metal coordination in self-assembly and mechanics of histidine-rich domains. European Polymer Journal, 2018, 109, 229-236.	5.4	26
354	Adaptations for Wear Resistance and Damage Resilience: Micromechanics of Spider Cuticular "Tools― Advanced Functional Materials, 2020, 30, 2000400.	14.9	26
355	Breaking of Rotational Symmetry during Decomposition of Elastically Anisotropic Alloys. Physical Review Letters, 1995, 75, 3458-3461.	7.8	25
356	Newly formed and remodeled human bone exhibits differences in the mineralization process. Acta Biomaterialia, 2020, 104, 221-230.	8.3	25
357	Honeycomb Actuators Inspired by the Unfolding of Ice Plant Seed Capsules. PLoS ONE, 2016, 11, e0163506.	2.5	25
358	Small-Angle Scattering of S-Layer Metallization. Advanced Materials, 2006, 18, 915-919.	21.0	24
359	Solving conflicting functional requirements by hierarchical structuring—Examples from biological materials. MRS Bulletin, 2016, 41, 667-671.	3.5	24
360	Ultrastructural, material and crystallographic description of endophytic masses – A possible damage response in shark and ray tessellated calcified cartilage. Journal of Structural Biology, 2017, 198, 5-18.	2.8	24

#	Article	IF	CITATIONS
361	The three-dimensional arrangement of the mineralized collagen fibers in elephant ivory and its relation to mechanical and optical properties. Acta Biomaterialia, 2018, 72, 342-351.	8.3	24
362	Mechanical properties of stingray tesserae: High-resolution correlative analysis of mineral density and indentation moduli in tessellated cartilage. Acta Biomaterialia, 2019, 96, 421-435.	8.3	24
363	Damage tolerance of lamellar bone. Bone, 2020, 130, 115102.	2.9	24
364	Spherulitic Crystal Growth Drives Mineral Deposition Patterns in Collagenâ€Based Materials. Advanced Functional Materials, 2022, 32, .	14.9	24
365	Volume fraction dependence of the structure function in Alî—,Ag. Acta Metallurgica Et Materialia, 1992, 40, 3381-3387.	1.8	23
366	Kinetics of joint ordering and decomposition in binary alloys. Physical Review B, 1997, 55, 2912-2919.	3.2	23
367	Digital image correlation shows localized deformation bands in inelastic loading of fibrolamellar bone. Journal of Materials Research, 2009, 24, 421-429.	2.6	23
368	Bioâ€Inspired Materials – Mining the Old Literature for New Ideas. Advanced Materials, 2010, 22, 4547-4550.	21.0	23
369	Hierarchically Structured Vanadium Pentoxide–Polymer Hybrid Materials. ACS Nano, 2014, 8, 5089-5104.	14.6	23
370	A Perfectly Periodic Threeâ€Dimensional Protein/Silica Mesoporous Structure Produced by an Organism. Advanced Materials, 2014, 26, 1682-1687.	21.0	22
371	The Geometric Design and Fabrication of Actuating Cellular Structures. Advanced Materials Interfaces, 2015, 2, 1500011.	3.7	22
372	From Beetles in Nature to the Laboratory: Actuating Underwater Locomotion on Hydrophobic Surfaces. Langmuir, 2015, 31, 13734-13742.	3.5	22
373	Ordering of protein and water molecules at their interfaces with chitin nano-crystals. Journal of Structural Biology, 2016, 193, 124-131.	2.8	22
374	Correlations between nanostructure and micromechanical properties of healing bone. Journal of the Mechanical Behavior of Biomedical Materials, 2018, 77, 258-266.	3.1	22
375	Epidermal Cell Surface Structure and Chitin–Protein Co-assembly Determine Fiber Architecture in the Locust Cuticle. ACS Applied Materials & Interfaces, 2020, 12, 25581-25590.	8.0	22
376	Microfibril Angles Inside and Outside Crossfields of Norway Spruce Tracheids. Holzforschung, 2003, 57, 13-20.	1.9	21
377	Semi-analytical approaches to assess the crack driving force in periodically heterogeneous elastic materials. International Journal of Fracture, 2012, 173, 57-70.	2.2	21
378	Selectivity in Bone Targeting with Multivalent Dendritic Polyanion Dye Conjugates. Advanced Healthcare Materials, 2014, 3, 375-385.	7.6	21

#	Article	IF	CITATIONS
379	Nano-channels in the spider fang for the transport of Zn ions to cross-link His-rich proteins pre-deposited in the cuticle matrix. Arthropod Structure and Development, 2017, 46, 30-38.	1.4	21
380	A new twist on sea silk: the peculiar protein ultrastructure of fan shell and pearl oyster byssus. Soft Matter, 2018, 14, 5654-5664.	2.7	21
381	Phase-separation kinetics of dilute Cu-Fe alloys studied by anomalous small-angle x-ray scattering and Mössbauer spectroscopy. Physical Review B, 1992, 46, 11323-11331.	3.2	20
382	Switching Mechanics with Chemistry: A Model for the Bending Stiffness of Amphiphilic Bilayers with Interacting Headgroups in Crystalline Order. Physical Review Letters, 2006, 97, 018106.	7.8	20
383	All but diamonds – Biological materials are not forever. Acta Materialia, 2013, 61, 880-889.	7.9	20
384	Effect of in vivo loading on bone composition varies with animal age. Experimental Gerontology, 2015, 63, 48-58.	2.8	20
385	Long bone maturation is driven by pore closing: A quantitative tomography investigation of structural formation in young C57BL/6 mice. Acta Biomaterialia, 2015, 22, 92-102.	8.3	20
386	Inherent Role of Water in Damage Tolerance of the Prismatic Mineral–Organic Biocomposite in the Shell of <i>Pinna Nobilis</i> . Advanced Functional Materials, 2016, 26, 3663-3669.	14.9	20
387	Breaking the long-standing morphological paradigm: Individual prisms in the pearl oyster shell grow perpendicular to the c-axis of calcite. Journal of Structural Biology, 2019, 205, 121-132.	2.8	20
388	Co-aligned chondrocytes: Zonal morphological variation and structured arrangement of cell lacunae in tessellated cartilage. Bone, 2020, 134, 115264.	2.9	20
389	Relation between the Macroscopic Pattern of Elephant Ivory and Its Three-Dimensional Micro-Tubular Network. PLoS ONE, 2017, 12, e0166671.	2.5	20
390	A neutron scattering investigation of the early stages of guinier-preston zone formation in AlZnMg(Cu)-alloys. Acta Metallurgica, 1982, 30, 547-552.	2.1	19
391	Monte Carlo simulation of diffusion in aB2-ordered model alloy. Physical Review B, 1998, 58, 3082-3088.	3.2	19
392	Tuning the Surface-Enhanced Raman Scattering Effect to Different Molecular Groups by Switching the Silver Colloid Solution pH. Applied Spectroscopy, 2009, 63, 214-223.	2.2	19
393	Synchrotron 3D SAXS analysis of bone nanostructure. Bioinspired, Biomimetic and Nanobiomaterials, 2012, 1, 123-131.	0.9	19
394	Defect-mediated nucleation of α-iron in Au-Fe alloys. Physical Review B, 1991, 44, 4192-4199.	3.2	18
395	Long-term correlations distinguish coarsening mechanisms in alloys. Physical Review B, 2003, 68, .	3.2	18
396	Effect of phosphorylation on the interaction of calcium with leucineâ€rich amelogenin peptide. European Journal of Oral Sciences, 2011, 119, 97-102.	1.5	18

#	Article	IF	CITATIONS
397	Measuring the distribution of cellulose microfibril angles in primary cell walls by small angle X-ray scattering. Plant Methods, 2014, 10, 25.	4.3	18
398	Magnetic force imaging of a chain of biogenic magnetite and Monte Carlo analysis of tip–particle interaction. Journal Physics D: Applied Physics, 2014, 47, 235403.	2.8	18
399	Ultrasonically Produced Porous Sponge Layer on Titanium to Guide Cell Behavior. Advanced Engineering Materials, 2016, 18, 476-483.	3.5	18
400	Wood made denser and stronger. Nature, 2018, 554, 172-173.	27.8	18
401	Internal oxidation of Cuî—,Fe—I. Small angle x-ray scattering study of oxide precipitation. Acta Metallurgica Et Materialia, 1994, 42, 2019-2026.	1.8	17
402	Microcracks and Osteoclast Resorption Activity In Vitro. Calcified Tissue International, 2012, 90, 230-238.	3.1	17
403	Hierarchical Structuring of Liquid Crystal Polymer–Laponite Hybrid Materials. Langmuir, 2013, 29, 11093-11101.	3.5	17
404	Nano―to Macroscale Remodeling of Functional Tissueâ€Engineered Bone. Advanced Healthcare Materials, 2013, 2, 546-551.	7.6	17
405	Influence of sacrificial bonds on the mechanical behaviour of polymer chains. Bioinspired, Biomimetic and Nanobiomaterials, 2014, 3, 139-145.	0.9	17
406	Chemical, colloidal and mechanical contributions to the state of water in wood cell walls. New Journal of Physics, 2016, 18, 083048.	2.9	17
407	Combined Experimental and Theoretical Approach to the Kinetics of Magnetite Crystal Growth from Primary Particles. Journal of Physical Chemistry Letters, 2017, 8, 1132-1136.	4.6	17
408	Ultrasound-driven titanium modification with formation of titania based nanofoam surfaces. Ultrasonics Sonochemistry, 2017, 36, 146-154.	8.2	17
409	Shape-preserving erosion controlled by the graded microarchitecture of shark tooth enameloid. Nature Communications, 2020, 11, 5971.	12.8	17
410	Microenvironment-mediated cancer dormancy: Insights from metastability theory. Proceedings of the National Academy of Sciences of the United States of America, 2022, 119, .	7.1	17
411	A 3D Network of Nanochannels for Possible Ion and Molecule Transit in Mineralizing Bone and Cartilage. Advanced NanoBiomed Research, 2022, 2, .	3.6	17
412	Volume-fraction dependence of the scaling function for phase-separating systems. Journal of Applied Crystallography, 1991, 24, 593-597.	4.5	16
413	Growth of Ordered Domains in a Computer Model Alloy with Lattice Misfit. Journal of Statistical Physics, 1999, 95, 23-43.	1.2	16
414	Coarsening in the Ising model with vacancy dynamics. Physica A: Statistical Mechanics and Its Applications, 2000, 279, 100-109.	2.6	16

#	Article	lF	CITATIONS
415	Microscopic computer simulations of directional coarsening in face-centered cubic alloys. Acta Materialia, 2001, 49, 53-63.	7.9	16
416	Effect of minimal defects in periodic cellular solids. Philosophical Magazine, 2010, 90, 1807-1818.	1.6	16
417	Early diagenesis of elephant tusk in marine environment. Palaeogeography, Palaeoclimatology, Palaeoecology, 2014, 416, 120-132.	2.3	16
418	The Mechanism of Color Change in the Neon Tetra Fish: a Lightâ€Induced Tunable Photonic Crystal Array. Angewandte Chemie, 2015, 127, 12603-12607.	2.0	16
419	The role of water on the structure and mechanical properties of a thermoplastic natural block co-polymer from squid sucker ring teeth. Bioinspiration and Biomimetics, 2016, 11, 055003.	2.9	16
420	<i>Fkbp10</i> Deletion in Osteoblasts Leads to Qualitative Defects in Bone. Journal of Bone and Mineral Research, 2017, 32, 1354-1367.	2.8	16
421	Mobility of hydrous species in amorphous calcium/magnesium carbonates. Physical Chemistry Chemical Physics, 2018, 20, 19682-19688.	2.8	16
422	Melorheostotic Bone Lesions Caused by Somatic Mutations in <i>MAP2K1</i> Have Deteriorated Microarchitecture and Periosteal Reaction. Journal of Bone and Mineral Research, 2019, 34, 883-895.	2.8	16
423	Protecting Offspring Against Fire: Lessons From Banksia Seed Pods. Frontiers in Plant Science, 2019, 10, 283.	3.6	16
424	Quantitative Backscattered Electron Imaging of Bone Using a Thermionic or a Field Emission Electron Source. Calcified Tissue International, 2021, 109, 190-202.	3.1	16
425	Experimental Observation of a Time-Scaling Characteristic in Alloy Decomposition in the AlZnMg System. Physical Review Letters, 1983, 51, 288-291.	7.8	15
426	Nanoscale Mechanisms of Bone Deformation and Fracture. , 0, , 397-414.		15
427	<i>In Situ</i> Imaging of Barnacle (<i>Balanus amphitrite</i>) Cyprid Cement Using Confocal Raman Microscopy. Journal of Adhesion, 2009, 85, 139-151.	3.0	15
428	A Composite Matter of Alignment. Science, 2012, 335, 177-178.	12.6	15
429	The role of topology and thermal backbone fluctuations on sacrificial bond efficacy in mechanical metalloproteins. New Journal of Physics, 2014, 16, 013003.	2.9	15
430	Mechanical behavior of idealized, stingray-skeleton-inspired tiled composites as a function of geometry and material properties. Journal of the Mechanical Behavior of Biomedical Materials, 2017, 73, 86-101.	3.1	15
431	Mechanoregulation of Bone Remodeling and Healing as Inspiration for Self-Repair in Materials. Biomimetics, 2019, 4, 46.	3.3	15
432	Model for the structural changes occurring at low temperatures inPdDx. II. Extension to lower concentrations. Physical Review B, 1981, 24, 6486-6490.	3.2	14

#	Article	IF	CITATIONS
433	The Heterogeneous Mineral Content of Bone—Using Stochastic Arguments and Simulations to Overcome Experimental Limitations. Journal of Statistical Physics, 2011, 144, 316-331.	1.2	14
434	Trabecular bone remodelling simulated by a stochastic exchange of discrete bone packets from the surface. Journal of the Mechanical Behavior of Biomedical Materials, 2011, 4, 879-887.	3.1	14
435	Enhancing low cost stainless steel implants: bioactive silica-based sol-gel coatings with wollastonite particles. International Journal of Nano and Biomaterials, 2012, 4, 33.	0.1	14
436	Nanostructure of Biogenic Calcite and Its Modification under Annealing: Study by High-Resolution X-ray Diffraction and Nanoindentation. Crystal Growth and Design, 2014, 14, 5275-5282.	3.0	14
437	Availability of extracellular matrix biopolymers and differentiation state of human mesenchymal stem cells determine tissue-like growth inÁvitro. Biomaterials, 2015, 60, 121-129.	11.4	14
438	Recombinant engineering of reversible cross-links into a resilient biopolymer. Polymer, 2015, 69, 255-263.	3.8	14
439	A new treatment of transient grain growth. Acta Materialia, 2016, 115, 442-447.	7.9	14
440	Impregnation and Swelling of Wood with Salts: Ion Specific Kinetics and Thermodynamics Effects. Advanced Materials Interfaces, 2017, 4, 1600437.	3.7	14
441	High-Performance All-Bio-Based Laminates Derived from Delignified Wood. ACS Sustainable Chemistry and Engineering, 2021, 9, 9638-9646.	6.7	14
442	The spider cuticle: a remarkable material toolbox for functional diversity. Philosophical Transactions Series A, Mathematical, Physical, and Engineering Sciences, 2021, 379, 20200332.	3.4	14
443	Adaptation of <i>Escherichia coli</i> Biofilm Growth, Morphology, and Mechanical Properties to Substrate Water Content. ACS Biomaterials Science and Engineering, 2021, 7, 5315-5325.	5.2	14
444	Breast Cancer Screening Using Small-Angle X-ray Scattering Analysis of Human Hair. Journal of the National Cancer Institute, 2000, 92, 1092-1093.	6.3	13
445	Surface-Directed Spinodal Decomposition on a Macroscopic Scale in a Nitrogen and Carbon Alloyed Steel. Physical Review Letters, 2003, 91, 015701.	7.8	13
446	Quantifying degradation of collagen in ancient manuscripts: the case of the Dead Sea Temple Scroll. Analyst, The, 2013, 138, 5594-5599.	3.5	13
447	Effect of collagen packing and moisture content on leather stiffness. Journal of the Mechanical Behavior of Biomedical Materials, 2019, 90, 1-10.	3.1	13
448	Multi-scale modeling and mechanical performance characterization of stingray skeleton-inspired tessellations. Journal of the Mechanics and Physics of Solids, 2020, 138, 103906.	4.8	13
449	The Earth's Lithosphere Inspires Materials Design. Advanced Materials, 2021, 33, 2005473.	21.0	13
450	Monte Carlo simulations of Mössbauer spectra in diffusion investigations. Physical Review B, 1999, 59, 8622-8625.	3.2	12

#	Article	IF	CITATIONS
451	Diffracting "stacks of cardsâ€+ some thoughts about small-angle scattering from bone. , 2005, , 33-39.		12
452	Onsager's coefficients and diffusion laws—a Monte Carlo study. Philosophical Magazine, 2005, 85, 1243-1260.	1.6	12
453	Relationship between nanoscale mineral properties and calcein labeling in mineralizing bone surfaces. Connective Tissue Research, 2014, 55, 15-17.	2.3	12
454	Nanocrystalline Calcitic Lens Arrays Fabricated by Self-Assembly Followed by Amorphous-to-Crystalline Phase Transformation. ACS Nano, 2014, 8, 9233-9238.	14.6	12
455	Hydro-actuation of ice plant seed capsules powered by water uptake. Bioinspired, Biomimetic and Nanobiomaterials, 2014, 3, 169-182.	0.9	12
456	Energy dissipation and recovery in a simple model with reversible cross-links. Physical Review E, 2015, 91, 032603.	2.1	12
457	Extra dimension for bone analysis. Nature, 2015, 527, 308-309.	27.8	12
458	Effect of Strontium Ions on Crystallization of Amorphous Calcium Carbonate. Crystal Research and Technology, 2019, 54, 1900002.	1.3	12
459	Hypermineralization in the femoral neck of the elderly. Acta Biomaterialia, 2019, 89, 330-342.	8.3	12
460	Collagen Pentablock Copolymers Form Smectic Liquid Crystals as Precursors for Mussel Byssus Fabrication. ACS Nano, 2021, 15, 6829-6838.	14.6	12
461	Hierarchical Structure and Repair of Bone: Deformation, Remodelling, Healing. Springer Series in Materials Science, 2007, , 323-335.	0.6	12
462	Reply to â€~ã€~Comment on â€~Kinetics of spinodal decomposition in the Ising model with vacancy diffusion' Physical Review B, 1996, 53, 2890-2891.	''. 3.2	11
463	On energy changes due to the formation of a circular hole in an elastic plate. Archive of Applied Mechanics, 2006, 76, 681-697.	2.2	11
464	Eshelby Twist as a Possible Source of Lattice Rotation in a Perfectly Ordered Protein/Silica Structure Grown by a Simple Organism. Small, 2015, 11, 5636-5641.	10.0	11
465	Electron microscope analyses of the bio-silica basal spicule from the Monorhaphis chuni sponge. Journal of Structural Biology, 2015, 191, 165-174.	2.8	11
466	Making a tooth mimic. Nature Materials, 2015, 14, 1082-1083.	27.5	11
467	Dendritic polyglycerol anions for the selective targeting of native and inflamed articular cartilage. Journal of Materials Chemistry B, 2017, 5, 4754-4767.	5.8	11
468	Temperature-induced self-sealing capability of <i>Banksia</i> follicles. Journal of the Royal Society Interface, 2018, 15, 20180190.	3.4	11

#	Article	IF	CITATIONS
469	Unraveling the Rapid Assembly Process of Stiff Cellulosic Fibers from Mistletoe Berries. Biomacromolecules, 2019, 20, 3094-3103.	5.4	11
470	Rapid collagen-directed mineralization of calcium fluoride nanocrystals with periodically patterned nanostructures. Nanoscale, 2021, 13, 8293-8303.	5.6	11
471	Hierarchical Structure and Mechanical Adaptation of Biological Materials. , 2004, , 15-34.		11
472	Lattice deformation inTaTxsystems due toHe3production. Physical Review B, 1986, 34, 4985-4988.	3.2	10
473	Local mechanical properties of tensile-deformed Al-8.4 at.%Li alloys examined by nanoindentation under an atomic force microscope. Scripta Materialia, 2000, 43, 15-20.	5.2	10
474	Thermodynamic modeling of a phase transformation in protein filaments with mechanical function. New Journal of Physics, 2013, 15, 065004.	2.9	10
475	Human and mouse bones physiologically integrate in a humanized mouse model while maintaining species-specific ultrastructure. Science Advances, 2020, 6, .	10.3	10
476	Synthesis of monodisperse rod-shaped silica particles through biotemplating of surface-functionalized bacteria. Nanoscale, 2020, 12, 8732-8741.	5.6	10
477	p53 influences mice skeletal development. Journal of Craniofacial Genetics and Developmental Biology, 1997, 17, 161-71.	0.1	10
478	Structure investigation of intelligent aerogels. Physica B: Condensed Matter, 2000, 276-278, 392-393.	2.7	9
479	Energy Dissipation and Stability of Propagating Surfaces. Physical Review Letters, 2005, 95, 195702.	7.8	9
480	Composition and Mechanical Properties of a Protein/Silica Hybrid Material Forming the Micronâ€Thick Axial Filament in the Spicules of Marine Sponges. Advanced Engineering Materials, 2014, 16, 1073-1077.	3.5	9
481	The virtues of tiling. Nature, 2014, 516, 178-179.	27.8	9
482	Registering 2D and 3D imaging data of bone during healing. Connective Tissue Research, 2015, 56, 133-143.	2.3	9
483	Function by internal structure–preface to the special issue on bioinspired hierarchical materials. Bioinspiration and Biomimetics, 2016, 11, 060301.	2.9	9
484	Preface to the proceedings of the 12th international conference on the chemistry and biology of mineralized tissues. Connective Tissue Research, 2018, 59, 1-5.	2.3	9
485	Interplay between mineral crystallinity and mineral accumulation in health and postmenopausal osteoporosis. Acta Biomaterialia, 2021, 124, 374-381.	8.3	9
486	Advanced materials design based on waste wood and bark. Philosophical Transactions Series A, Mathematical, Physical, and Engineering Sciences, 2021, 379, 20200345.	3.4	9

#	Article	IF	CITATIONS
487	An Experimental Study of the Role of Plasticity in the Rafting Kinetics of a Single Crystal Ni-Base Superalloy. , 1996, , .		9
488	Alloy decomposition in Cu-Ni-Fe. II. Decomposition and coarsening of periodic structures. Journal of Physics F: Metal Physics, 1986, 16, 1905-1916.	1.6	8
489	Lattice dynamics and phonon line shapes ofPd0.9Ag0.1D0.61at 100 K. Physical Review B, 1986, 34, 164-168.	3.2	8
490	Phase boundary structure of γ′-particles in Cu-10 at.% Be. Acta Metallurgica Et Materialia, 1995, 43, 1305-1311.	1.8	8
491	Strain-induced morphologies during homogeneous phase separation in alloys. Phase Transitions, 1999, 67, 707-724.	1.3	8
492	Serrated flow and related microstructures in an Al-8.4 at.% Li alloy. Journal of Materials Science, 2002, 37, 1355-1361.	3.7	8
493	Mechanics of the Expanding Cell Wall. , 2006, , 191-215.		8
494	Mapping Dynamical Mechanical Properties of Osteonal Bone by Scanning Acoustic Microscopy in Time-of-Flight Mode. Microscopy and Microanalysis, 2014, 20, 924-936.	0.4	8
495	Reentrant phase transformation from crystalline ikaite to amorphous calcium carbonate. CrystEngComm, 2018, 20, 2902-2906.	2.6	8
496	Cortical bone properties in the Brtl/+ mouse model of Osteogenesis imperfecta as evidenced by acoustic transmission microscopy. Journal of the Mechanical Behavior of Biomedical Materials, 2019, 90, 125-132.	3.1	8
497	Spatiotemporal Measurement of Osmotic Pressures by FRET Imaging. Angewandte Chemie - International Edition, 2021, 60, 6488-6495.	13.8	8
498	Polyelectrolyte Substrate Coating for Controlling Biofilm Growth at Solid–Air Interface. Advanced Materials Interfaces, 2021, 8, 2001807.	3.7	8
499	Effects of moisture and cellulose fibril angle on the tensile properties of native single Norway spruce wood fibres. Wood Science and Technology, 2021, 55, 1305-1318.	3.2	8
500	Alterations of bone material properties in growing Ifitm5/BRIL p.S42 knock-in mice, a new model for atypical type VI osteogenesis imperfecta. Bone, 2022, 162, 116451.	2.9	8
501	Investigation of cluster growth in Al-Zn-Mg systems with analysis of time-scaling properties. Physical Review B, 1984, 30, 6498-6503.	3.2	7
502	Formation of a Modulated Void Structure in Heavy-Ion-Irradiated Amorphous Silicon. Europhysics Letters, 1990, 11, 547-553.	2.0	7
503	A new stretching apparatus for applying anisotropic mechanical strain to bone cellsin-vitro. Review of Scientific Instruments, 2000, 71, 3522-3529.	1.3	7
504	Mineral crystal alignment in mineralized fracture callus determined by 3D small-angle X-ray scattering. Journal of Physics: Conference Series, 2010, 247, 012031.	0.4	7

#	Article	IF	CITATIONS
505	Mapping Lattice Spacing and Composition in Biological Materials by Means of Microbeam Xâ€Ray Diffraction. Advanced Engineering Materials, 2011, 13, 784-792.	3.5	7
506	Imaging Mineralized Tissues in Vertebrates. , 2011, , 407-426.		7
507	Gas barrier properties of bio-inspired Laponite–LC polymer hybrid films. Bioinspiration and Biomimetics, 2016, 11, 035005.	2.9	7
508	Heterogeneity of the osteocyte lacuno-canalicular network architecture and material characteristics across different tissue types in healing bone. Journal of Structural Biology, 2020, 212, 107616.	2.8	7
509	Globular structure of the hypermineralized tissue in human femoral neck. Journal of Structural Biology, 2020, 212, 107606.	2.8	7
510	Bioinspired Compartmentalization Strategy for Coating Polymers with Self-Organized Prismatic Films. Chemistry of Materials, 2021, 33, 9240-9251.	6.7	7
511	Spiral angle of elementary cellulose fibrils in cell walls of Picea abies determined by small-angle X-ray scattering. Wood Science and Technology, 1998, 32, 335-345.	3.2	7
512	Interatomic Potentials and Lattice Distortions in PdD0.8*. Zeitschrift Fur Physikalische Chemie, 1985, 146, 159-169.	2.8	6
513	Radiation-induced segregation in proton-irradiated AuFe studied by Mossbauer spectroscopy. Journal of Physics Condensed Matter, 1992, 4, 2415-2428.	1.8	6
514	Experimental Evidence for Rhombohedral Phase of C 70 after Irradiation. Europhysics Letters, 1993, 22, 585-589.	2.0	6
515	Internal oxidation of Cuî—,Fe—II. The morphology of oxide inclusions from the minimization of elastic misfit energy. Acta Metallurgica Et Materialia, 1994, 42, 2027-2033.	1.8	6
516	Microscopic Diffusion Mechanism of Iron in FeAl Revisited by New Methods. Materials Research Society Symposia Proceedings, 1998, 527, 197.	0.1	6
517	Editorial. Bone, 1999, 24, 619-620.	2.9	6
518	Neurofibromin inactivation impairs osteocyte development in Nf1Prx1 and Nf1Col1 mouse models. Bone, 2014, 66, 155-162.	2.9	6
519	Self-healing silk from the sea: role of helical hierarchical structure in <i>Pinna nobilis</i> byssus mechanics. Soft Matter, 2019, 15, 9654-9664.	2.7	6
520	Distortion induced by helium formation in tantalum-tritium systems. Journal of Nuclear Materials, 1986, 141-143, 540-542.	2.7	5
521	Biologische Materialien ―dem Bauplan natürlicher Hochleistungswerkstoffe auf der Spur. Physik in Unserer Zeit, 1999, 30, 196-200.	0.0	5
522	Dynamics of mesoscopic precipitate lattices in phase-separating alloys under external load. Europhysics Letters, 2000, 52, 224-230.	2.0	5

#	Article	IF	CITATIONS
523	Regular, low density cellular structures - rapid prototyping, numerical simulation, mechanical testing. Materials Research Society Symposia Proceedings, 2004, 823, W8.8.1.	0.1	5
524	Relating Local Bone Stiffness and Calcium Content by Combined Nanoindentation and Backscattered Electron Imaging. Materials Research Society Symposia Proceedings, 2005, 874, 1.	0.1	5
525	Finite Element Modeling of the Cyclic Wetting Mechanism in the Active Part of Wheat Awns. Biointerphases, 2012, 7, 42.	1.6	5
526	The nanostructure of murine alveolar bone and its changes due to type 2 diabetes. Journal of Structural Biology, 2016, 196, 223-231.	2.8	5
527	Combining Coherent Hard X-Ray Tomographies with Phase Retrieval to Generate Three-Dimensional Models of Forming Bone. Frontiers in Materials, 2017, 4, .	2.4	5
528	Normal trabecular vertebral bone is formed via rapid transformation of mineralized spicules: A high-resolution 3D ex-vivo murine study. Acta Biomaterialia, 2019, 86, 429-440.	8.3	5
529	Mistletoe viscin: a hygro- and mechano-responsive cellulose-based adhesive for diverse material applications. , 2022, 1, .		5
530	Scaling properties of the D-short range order in PdDx for higher D concentrations. Solid State Communications, 1984, 51, 47-50.	1.9	4
531	Dissolution of precipitates heated above the solubility line: A Monte Carlo simulation. Physical Review B, 1997, 55, 12121-12127.	3.2	4
532	Nanoscale elastic modulus mapping revisited: The concept of effective mass. Journal of Applied Physics, 2014, 116, .	2.5	4
533	Lightâ€Induced Water Splitting Causes Highâ€Amplitude Oscillation of pHâ€5ensitive Layerâ€by‣ayer Assembl on TiO ₂ . Angewandte Chemie, 2016, 128, 13195-13198.	ies 2.0	4
534	Multiscale Analysis of Mineralized Collagen Combining X-ray Scattering and Fluorescence with Raman Spectroscopy under Controlled Mechanical, Thermal, and Humidity Environments. ACS Biomaterials Science and Engineering, 2017, 3, 2853-2859.	5.2	4
535	The Emergence of Complexity from a Simple Model for Tissue Growth. Journal of Statistical Physics, 2020, 180, 459-473.	1.2	4
536	Tomographic X-ray scattering based on invariant reconstruction: analysis of the 3D nanostructure of bovine bone. Journal of Applied Crystallography, 2021, 54, 486-497.	4.5	4
537	Sequence-specific response of collagen-mimetic peptides to osmotic pressure. MRS Bulletin, 2021, 46, 889-901.	3.5	4
538	Mechanical model for the deformation of the wood cell wall. International Journal of Materials Research, 2022, 95, 579-584.	0.3	4
539	Deuterium short-range order inPd0.975Ag0.025D0.685by diffuse neutron scattering. Physical Review B, 1983, 28, 3579-3581.	3.2	3
540	Shape and size of non-spherical particles in single crystals, investigated by SAXS. European Physical Journal Special Topics, 1993, 03, C8-325-C8-328.	0.2	3

#	Article	IF	CITATIONS
541	The Influence of the Thermal Treatment of Hydroxylapatite Scaffolds on the Physical Properties and the Bone Cell Ingrowth Behaviour. Materials Research Society Symposia Proceedings, 2005, 874, 1.	0.1	3
542	Fracture of poly(vinylidene fluoride): a combined synchrotron and laboratory in-situ X-ray scattering study. Journal of Applied Crystallography, 2007, 40, s564-s567.	4.5	3
543	Mesoporous Silica: A Perfectly Periodic Three-Dimensional Protein/Silica Mesoporous Structure Produced by an Organism (Adv. Mater. 11/2014). Advanced Materials, 2014, 26, 1681-1681.	21.0	3
544	Stress-mediated formation of nanocrystalline calcitic microlens arrays. CrystEngComm, 2015, 17, 9135-9141.	2.6	3
545	Tissue growth controlled by geometric boundary conditions: a simple model recapitulating aspects of callus formation and bone healing. Journal of the Royal Society Interface, 2015, 12, 20150108.	3.4	3
546	High resolution 3D laboratory x-ray tomography data of femora from young, 1–14 day old C57BL/6 mice. Data in Brief, 2015, 4, 32-33.	1.0	3
547	Twisters: An analogy of bilayers for twisting. Journal of the Mechanics and Physics of Solids, 2020, 134, 103742.	4.8	3
548	Complex Biological Structures: Collagen and Bone. Biological and Medical Physics Series, 2006, , 205-223.	0.4	3
549	Kinetics of Phase Separation Along Stable Trajectories. , 1988, , 223-231.		3
550	Self-organized rod undulations on pre-stretched textiles. Bioinspiration and Biomimetics, 2022, 17, 036007.	2.9	3
551	Heat-Mediated Micro- and Nano-pore Evolution in Sea Urchin Biominerals. Crystal Growth and Design, 2022, 22, 3727-3739.	3.0	3
552	Bone mineral structure after six years fluoride treatment investigated by backscattered electron imaging (BSEI) and small angle X-ray scattering (SAXS): A case report. Bone, 1995, 16, 407.	2.9	2
553	SAS experiments on inorganic gels. Physica B: Condensed Matter, 1997, 234-236, 279-280.	2.7	2
554	Title is missing!. Journal of Materials Science Letters, 2001, 20, 2245-2247.	0.5	2
555	Microscopic Diffusion Mechanisms in Fe-Al, Ni-Ga and (Ni Fe)-Al B2 Phases. Defect and Diffusion Forum, 2001, 194-199, 349-356.	0.4	2
556	Ein Knochenjob für die Biomimetik. Nachrichten Aus Der Chemie, 2007, 55, 644-646.	0.0	2
557	Inside Front Cover: Effects of Laminate Architecture on Fracture Resistance of Sponge Biosilica: Lessons from Nature (Adv. Funct. Mater. 8/2008). Advanced Functional Materials, 2008, 18, 1146-1146.	14.9	2

558 Vibrational spectroscopy in biomedical science: bone. , 2009, , .

#	Article	IF	CITATIONS
559	The evolution of size and distribution of apatite mineral crystals during bone fracture healing in sheep. Bone, 2009, 44, S271-S272.	2.9	2
560	Mechanical Function of a Complex Three-dimensional Suture Joining the Bony Elements in the Shell of the Red-eared Slider Turtle. Materials Research Society Symposia Proceedings, 2009, 1187, 19.	0.1	2
561	In-situ Raman Spectroscopic Imaging of a Mussel Coating and Adhesive. , 2010, , .		2
562	Collagen Orientation During Early Stages of Bone Fracture Healing Investigated by Polarized Raman Imaging. , 2010, , .		2
563	Functional mapping of bone on the micrometer-scale by scanning acoustic microscopy. Bone, 2012, 50, S125-S126.	2.9	2
564	Apatite alignment and orientation at the Ãngstrom and nanometer length scales shed light on the adaptation of dentine to whole tooth mechanical function. Bioinspired, Biomimetic and Nanobiomaterials, 2013, 2, 194-202.	0.9	2
565	Collagen. , 2016, , .		2
566	3.26 Imaging Mineralized Tissues in Vertebrates â~†. , 2017, , 549-578.		2
567	Data on collagen structures in leather with varying moisture contents from small angle X-ray scattering and three point bend testing. Data in Brief, 2018, 21, 1220-1226.	1.0	2
568	The effect of aging on the nanostructure of murine alveolar bone and dentin. Journal of Bone and Mineral Metabolism, 2021, 39, 757-768.	2.7	2
569	Scanning-SAXS: a tool for structural characterization of complex materials at the micrometer and the nanometer scale. Acta Crystallographica Section A: Foundations and Advances, 2002, 58, c25-c25.	0.3	2
570	Scanning X-ray scattering study on structural changes at crack tips in PVDF. Acta Crystallographica Section A: Foundations and Advances, 2005, 61, c391-c391.	0.3	2
571	Stable trajectories during decomposition of a dilute alloy. Physical Review B, 1987, 36, 2110-2114.	3.2	1
572	Pore evolution during sintering in molybdenum. Philosophical Magazine A: Physics of Condensed Matter, Structure, Defects and Mechanical Properties, 1987, 56, 615-624.	0.6	1
573	Anomalously Fast Diffusion of Fe in beta-ZrNb Alloy. Defect and Diffusion Forum, 1990, 66-69, 353-358.	0.4	1
574	Holz und Knochen — intelligente Werkstoffe der Natur. Physik Journal, 1995, 51, 1191-1192.	0.1	1
575	Bone mineral ultrastructure in humans and various mammals as investigated by small-angle x-ray scattering. Bone, 1995, 16, 399.	2.9	1
576	Nanostructure Analysis of Complex Materials using Two-Dimensional Small Angle X-Ray Scattering. Materials Science Forum, 2003, 414-415, 411-418.	0.3	1

#	Article	IF	CITATIONS
577	3D Small Angle X-Ray Scattering (SAXS) on deformed PVDF Foils. Materials Research Society Symposia Proceedings, 2003, 782, 1.	0.1	1
578	Collagen: Hierarchical Structure and Viscoelastic Properties of Tendon. , 2003, , 175-188.		1
579	Small-angle scattering from spherical particles on randomly oriented interfaces. International Journal of Materials Research, 2006, 97, 290-294.	0.8	1
580	Editorial for Biointerphases in focus: research on biointerfaces with neutrons and synchrotron radiation. Biointerphases, 2008, 3, FB1-FB2.	1.6	1
581	Mapping Nanomechanical Properties near Internal Interfaces in Biological Materials. Materials Research Society Symposia Proceedings, 2012, 1345, 1.	0.1	1
582	Evidence of polyphosphates and their distribution in active biological apatite mineralization sites of stingray jaws. Bone, 2012, 50, S99-S100.	2.9	1
583	Mineral particle size in children with dominant osteogenesis imperfecta is not associated with specific collagen mutation: A synchrotron X-ray scattering study. Bone, 2012, 50, S129.	2.9	1
584	Preface for the special issue celebrating Stephen Weiner's 65th birthday. Journal of Structural Biology, 2013, 183, 105-106.	2.8	1
585	The role of angular reflection in assessing elastic properties of bone by scanning acoustic microscopy. Journal of the Mechanical Behavior of Biomedical Materials, 2014, 29, 438-450.	3.1	1
586	An Introduction into the Physics of Self-folding Thin Structures. Science Studies, 2016, , 175-210.	0.0	1
587	Surface-Enhanced Raman Scattering Microspectroscopy Enables the Direct Characterization of Biomineral-Associated Organic Material on Single Calcareous Microskeletons. Journal of Physical Chemistry Letters, 2020, 11, 8623-8629.	4.6	1
588	Correlative Analysis of Specific Compatibilization in Composites by Coupling in situ X-Ray Scattering and Mechanical Tensile Testing. Frontiers in Materials, 2020, 6, .	2.4	1
589	Spatiotemporal Measurement of Osmotic Pressures by FRET Imaging. Angewandte Chemie, 2021, 133, 6562-6569.	2.0	1
590	Small-Angle Scattering of Synchrotron Radiation for Studying Solid State and Biological Systems. Acta Physica Polonica A, 1992, 82, 121-136.	0.5	1
591	Veräderungen des Kollagens bei Ho: YAG-Laserthermokeratoplastik. , 1994, , 574-578.		1
592	Strain and Shape in Self-Assembled Quantum Dots Studied by X-Ray Grazing Incidence Diffraction. Materials Research Society Symposia Proceedings, 1998, 524, 89.	0.1	0
593	Short- and intermediate-range structure in Al(III)-containing gels prepared from Al-nitrate in organic medium. Chemical Physics, 1999, 246, 295-305.	1.9	0
594	Structure and mechanics of muscle and tendon. Synchrotron Radiation News, 2002, 15, 18-26.	0.8	0

#	Article	IF	CITATIONS
595	Small Angle X-Ray Scattering with Cobalt Radiation for Nanostructure Characterization of Fe-Based Specimen. Materials Science Forum, 2004, 443-444, 155-158.	0.3	0
596	Time- and position-resolved X-ray scattering of bone and cartilage. Acta Crystallographica Section A: Foundations and Advances, 2005, 61, c123-c123.	0.3	0
597	Architectural changes of trabecular bone caused by the remodeling process. Materials Research Society Symposia Proceedings, 2005, 874, 1.	0.1	0
598	Phase Separation in Binary Alloys - Modeling Approaches. , 2004, , 57-116.		0
599	Towards understanding of trabecular bone failure by deformation localisation. Bone, 2008, 42, S49.	2.9	0
600	Cortical bone orientation and composition in a mouse model as a function of tissue age vs animal age. Bone, 2009, 44, S269-S270.	2.9	0
601	In-situ Damage Assessment of Collagen within Ancient Manuscripts Written on Parchment: A Polarized Raman Spectroscopy Approach. , 2010, , .		0
602	Hybrid Materials: An Alternative Route Towards Metal–Polymer Hybrid Materials Prepared by Vaporâ€Phase Processing (Adv. Funct. Mater. 16/2011). Advanced Functional Materials, 2011, 21, 3002-3002.	14.9	0
603	Multi-Method 3D Characterization of Different Tissue Types in Healing Bone. Microscopy and Microanalysis, 2019, 25, 358-359.	0.4	0
604	Hierarchical structure of bone and wood studied by scanning X-ray scattering. Acta Crystallographica Section A: Foundations and Advances, 2000, 56, s70-s70.	0.3	0
605	Scanning texture analysis of lamellar bone using microbeam synchrotron radiation. Acta Crystallographica Section A: Foundations and Advances, 2005, 61, c311-c311.	0.3	0
606	Microbeam diffraction of hierarchical nanocomposites. Acta Crystallographica Section A: Foundations and Advances, 2005, 61, c63-c64.	0.3	0
607	Materials research with scanning microfocus small-angle X-ray scattering. Acta Crystallographica Section A: Foundations and Advances, 2008, 64, C10-C10.	0.3	0
608	Materials Science Aspects of Bone Fracture and Regeneration. IFMBE Proceedings, 2009, , 259-259.	0.3	0
609	Role of amelogenin self-assembly in protein-mediated dental enamel formation. , 2010, , 369-374.		0
610	Small-angle scattering from spherical particles on randomly oriented interfaces. International Journal of Materials Research, 2022, 97, 290-294.	0.3	0
611	Spatial correlations between the local architecture of the lacunocanalicular network and the surrounding mineralized matrix in mouse tibiae. Bone Reports, 2022, 16, 101335.	0.4	0